

1 Multifactorial effects of warming, low irradiance, and low salinity on Arctic kelps

2 Anaïs Lebrun<sup>1</sup>, Cale A. Miller<sup>1,2</sup>, Marc Meynadier<sup>3</sup>, Steeve Comeau<sup>1</sup>, Pierre Urrutti<sup>1</sup>, Samir  
3 Alliouane<sup>1</sup>, Robert Schlegel<sup>1</sup>, Jean-Pierre Gattuso<sup>1,4</sup>, Frédéric Gazeau<sup>1</sup>

4 <sup>1</sup> Laboratoire d'Océanographie de Villefranche, Sorbonne Université, CNRS, Villefranche-sur-  
5 Mer, France

6 <sup>2</sup> Department of Earth Sciences, Utrecht University, Utrecht, The Netherlands

7 <sup>3</sup> Laboratoire de Biologie du Développement de Villefranche-sur-Mer, Sorbonne Université,  
8 CNRS, Villefranche-sur-Mer, France

9 <sup>4</sup> Institute for Sustainable Development and International Relations, Sciences Po, Paris, France

## 11 Abstract

12 The Arctic is projected to warm by 2 to 5°C by the end of the century. Warming causes melting of  
13 glaciers, shrinking of the areas covered by sea ice, and increased terrestrial runoff from snowfields  
14 and permafrost thawing. Warming, decreasing coastal underwater irradiance, and lower salinity  
15 are potentially threatening polar marine organisms, including kelps, that are key species of hard-  
16 bottom shallow communities. The present study investigates the physiological responses of four  
17 kelp species (*Alaria esculenta*, *Laminaria digitata*, *Saccharina latissima*, and *Hedophyllum*  
18 *nigripes*) to these environmental changes through a perturbation experiment in *ex situ* mesocosms.

19 Kelps were exposed for six weeks to four experimental treatments: an unmanipulated control, a  
20 warming condition under the CO<sub>2</sub> emission scenario SSP5-8.5, and two multifactorial conditions  
21 combining warming, low salinity, and low irradiance reproducing the future coastal Arctic exposed  
22 to terrestrial runoff under two CO<sub>2</sub> emission scenarios (SSP2-4.5 and SSP5-8.5). The

23 physiological effects on *A. esculenta*, *L. digitata* and *S. latissima* were investigated and gene  
24 expression patterns of *S. latissima* and *H. nigripes* were analyzed. Across all species and  
25 experimental treatments, growth rates were similar, underlying the acclimation potential of these  
26 species to future Arctic conditions. Specimens of *A. esculenta* increased their chlorophyll *a* content  
27 when exposed to low irradiance conditions, suggesting that they may be resilient to an increase in  
28 glacier and river runoff with the potential to become more dominant at greater depths. *S. latissima*  
29 showed a lower carbon:nitrogen (C:N) ratio under the SSP5-8.5 multifactorial conditions  
30 treatment, suggesting tolerance to coastal erosion and permafrost thawing. In contrast, *L. digitata*  
31 showed no response to the conditions tested on any of the investigated physiological parameters.

32 The down-regulation of genes coding for heat-shock proteins in *H. nigripes* and *S. latissima*

Deleted: m

Deleted: warming, low irradiance, and low salinity

Deleted: conducted

Deleted: during

Deleted: mimicking future coastlines unimpacted by glacier melting ...

Deleted: following

Deleted: resilience

Deleted: each

Deleted: '

Deleted: acclimation potential

Deleted: and

Deleted: at higher nitrate concentrations

Deleted: could benefit the organism in the future Arctic

Deleted: s

Deleted: gene expression

Deleted: patterns

Deleted: s of

51 underscores their ability to acclimate to heat stress, which portrays temperature as a key  
52 influencing factor. Based on these results, it is expected that kelp communities will undergo  
53 changes in species composition that will vary at local scale as a function of the changes in  
54 environmental drivers.

55  
56 Keywords: climate change - Arctic - kelps - mesocosm  
57

### 58 Summary (500 characters)

59 We tested the effects of warming, low salinity, and low irradiance on Arctic kelps. We show that  
60 growth rates were similar across species and treatments. *Alaria esculenta* is adapted to low light  
61 conditions. *Saccharina latissima* exhibited nitrogen limitation suggesting coastal erosion and  
62 permafrost thawing could be beneficial. *Laminaria digitata* did not respond to the treatments. Gene  
63 expression of *Hedophyllum nigripes* and *S. latissima* indicated acclimation to the experimental  
64 treatments.

### 65 66 1. Introduction

67 The Arctic region is warming at more than twice the global average rate (Richter-Menge et al.,  
68 2017). Over the next 80 years, sea surface temperature is projected to increase by 2°C according  
69 to the Shared Socio-economic Pathways (SSP) 1-2.6, which foresees an increasing shift towards  
70 sustainable practices, and up to 5°C according to the SSP5-8.5, which assumes an energy-intensive  
71 and fossil fuel-based economy (Kwiatkowski et al., 2020). Warming induces glacier and sea ice  
72 to melt at a faster rate causing an increase in terrestrial runoff from thawing snowfields and  
73 permafrost (Shiklomanov and Shiklomanov 2003; Stroeve et al., 2014). Total freshwater inflow  
74 into the Arctic Ocean rose by around 7% between 1936 and 1999 and 14% between 1980 and 2009  
75 (Peterson et al., 2002; Ahmed et al., 2020). Combined with vertical mixing by waves and wind  
76 action, cryosphere melting results in local turbid and low-salinity waters down to 20 m (Karsten  
77 2007). Coastal areas are therefore exposed to warming, changing light and salinity conditions  
78 (Lebrun et al., 2022).

79 In the coastal Arctic, kelps are key ecosystem engineers that form underwater forests. Kelp  
80 are large brown macroalgae of the class Phaeophyceae and the order Laminariales. Kelp forests  
81 provide a food source, habitat, and nursery ground for numerous fish and invertebrates as well as  
82 protection of coastlines from erosion (Filbee-Dexter et al., 2019). They support complex food webs  
83 and have a substantial role in storing and sequestering carbon (Krause-Jensen and Duarte 2016).

Deleted: ability

Deleted: acclimate

Deleted:

Deleted: and underline

Deleted:

Deleted:

Deleted: For future research, potential cascading effects on the associated fauna and the whole ecosystem are important to anticipate the ecological, cultural, and economic impacts of climate change in the Arctic.

Deleted: G

Deleted: , which might explain why it is becoming dominant at depth...

Deleted: it it

Deleted:

Deleted: s

Formatted: Indent: First line: 0.5"

Deleted: Phaeophyceae

Deleted: , respectively

Deleted: the

103 *Saccharina latissima*, *Alaria esculenta*, *Laminaria digitata*, and *Hedophyllum nigripes* are four  
104 abundant kelp species that inhabit the northern hemisphere and extend to subarctic and Arctic  
105 waters (Bischof et al., 1999; Müller et al. 2009). As a result of warming, which induces more sea  
106 ice-free areas, the surface area suitable for kelps has increased by about 45% from 1940-1950 to  
107 2000-2017 (Krause-Jensen et al., 2020). Temperature requirements and seasonal variability  
108 tolerance in irradiance and salinity for reproduction and growth determine the geographical  
109 distribution of kelp species (Wiencke et al. 1994, Muth et al., 2021). The temperature tolerance of  
110 these kelp species found in the Arctic appears broad (0 - 20°C), however, there is significant  
111 variability in temperature optima across ecotypes (Bolton and Lüning, 1982, Andersen et al., 2013,  
112 Diehl et al., 2021). Similarly, low salinity is well tolerated (Karsten et al. 2007), yet it is unclear  
113 how low salinity stress may interact with other stressors. Irradiance has a major impact on their  
114 depth distribution (e.g. Roleda et al. 2005; Krause-Jensen et al., 2012). Turbid waters alter kelp  
115 fitness by limiting photosynthesis. This has already induced a shift in the vertical distribution of  
116 kelps such as *Laminaria* and *Saccharina* genera to shallower waters in Arctic fjords (Bartsch et  
117 al., 2016; Filbee-Dexter et al., 2019). Because optimal temperature, irradiance, and salinity ranges  
118 vary between kelp species, their response to environmental changes will likely be species-specific  
119 (Eggert 2012; Karsten 2012).

120 We hypothesized that (1) warming will enhance the growth rate of Arctic kelps in  
121 Kongsfjorden during summer, and (2) that the combined effects of high temperature, low salinity  
122 and low irradiance will negatively impact their physiology, although responses will be species-  
123 specific. To test these hypotheses and fill knowledge gaps on the multifactorial effects of climate  
124 change across species (Renaud et al., 2019; Scherrer et al., 2019), we carried out a land-based  
125 mesocosm experiment exposing four kelp species (*S. latissima*, *A. esculenta*, *L. digitata*, and *H.*  
126 *nigripes*), found in common biomass between 5 to 10 m depth to four treatments for six weeks.  
127 The treatments consisted of a control, a warming condition mimicking the future offshore (T1),  
128 and two multifactorial conditions combining warming, low salinity, and low irradiance mimicking  
129 the future coastal Arctic (T2 and T3). In order to best represent *in situ* conditions, the different  
130 kelp species were incubated together in each mesocosm at densities mimicking natural  
131 communities. The physiological effects on *A. esculenta*, *L. digitata* and *S. latissima* were  
132 investigated and gene expression patterns of *S. latissima* and *H. nigripes* were analyzed.

Deleted:

Deleted: significant

Deleted:

Deleted: Andersen et al., 2013;

Deleted: ;

Deleted: (Bolton and Luning 1982, Andersen et al. 2013, Diehl et al. 2021)

Deleted: yet,

Deleted:

Deleted: density

143 **2. Material and methods**

144 **2.1 Specimen collection**

145 In June 2021, 188 sporophytes of *A. esculenta*, *L. digitata*, *S. latissima*, and *H. nigripes* shorter  
146 than 1 m were collected by research divers in Kongsfjorden (Svalbard, Norway). They were  
147 collected between 2 and 7 m depth at Hansneset and the Old Pier (Fig. 1). All samples were placed  
148 into holding tanks ( $\geq 1 \text{ m}^3$ ) with flow-through ambient seawater until their placement into final  
149 mesocosms on 2021-07-03.

150

151 **2.2 Mesocosm experiment**

152 The experiment was carried out from 2021-07-03 ( $t_0$ ) to 2021-08-28 ( $t_{\text{final}}$ ), in twelve  $1 \text{ m}^3$   
153 mesocosms set up in Ny-Ålesund on the outdoor platform of the Kings Bay Marine Laboratory in  
154 order to expose communities to natural light cycles. Each mesocosm received 3 to 6 individuals  
155 of *A. esculenta* and *S. latissima*, 2 to 4 individuals of *L. digitata* and 0 to 2 individuals of *H.*  
156 *nigripes* for a total kelp biomass (wet weight) per mesocosm of about 1500 g for *S. latissima* and  
157 *L. digitata* (mingled with *H. nigripes*) and 1000 g for *A. esculenta*. These biomasses are  
158 representative of those found at Hansneset down to 7 m depth (Hop et al., 2012). Since *H. nigripes*  
159 can be mistaken for *L. digitata*, each stipe of these two species was cut at  $t_{\text{final}}$  to detect individuals  
160 with mucilage, corresponding to *H. nigripes* ( $n=16$ , Dankworth et al., 2020).

161 The experimental set-up is briefly described below. More information can be found in  
162 Miller et al. (2024a). Seawater flowing through the mesocosms was pumped from 10 m depth in  
163 front of the Kings Bay Marine Laboratory (78.929°N, 11.930°E) using a submersible pump  
164 (Albatros©). The regulated flow-through system ( $7 - 8 \text{ L min}^{-1}$  in each mesocosm) allowed for  
165 the automated control of temperature and salinity. Temperature was adjusted by mixing ambient  
166 seawater with warmed seawater ( $15^\circ\text{C}$ ) and salinity was regulated by addition of freshwater.

167 Irradiance was modified by placing spectra and attenuating light filters on top of each mesocosm  
168 to simulate current irradiance and future *in situ* irradiance (see below for more details). Each  
169 mesocosm was equipped with one 12 W wave pump (Sunsun© JVP-132) to ensure proper mixing.

170 Four experimental treatments in triplicate (4x3 mesocosms) were used to study conditions  
171 representative of present and future Arctic coastal communities at proximity or not to glaciers  
172 following two different SSP scenarios (Ctrl, T1, T2, T3; Table 1). Treatments 1 and 2 (T1 and T2)  
173 mimicked the conditions expected close to glaciers and, therefore, combined warming, low  
174 irradiance, and low salinity. T1 followed the SSP 2-4.5, which describes a middle-of-the-road  
175 projection that does not shift markedly from historical patterns, while T2 followed the SSP5-8.5

Formatted: Font: Bold

Formatted: Font: Bold

Deleted:

Formatted: Font: Bold

Formatted: Font: Bold

Deleted: mass (wet weight) of

Formatted: Indent: First line: 0.5"

Deleted: under revision

Deleted: Each mesocosm was equipped with one 12 W wave pump (Sunsun© JVP-132) to ensure proper mixing.

Deleted: over top

182 that assumes an energy-intensive and fossil fuel-based economy. T3 focused on the projected  
183 change outside glacial fjords following the SSP 5-8.5, where warming acts as a single driver.  
184 Temperature was increased by 3.3°C in T1 and 5.3°C in T2 and T3 as an offset increase from the  
185 control condition (Ctrl) which mimicked the *in situ* temperature recorded in real-time during the  
186 whole experiment. Based on *in situ* measurements of temperature and salinity in Kongsfjorden  
187 taken from week 22 to 35 in 2020, salinity offsets were determined from the *in situ* relationship  
188 between temperature, salinity and extrapolated to apply to future warming. This resulted in a  
189 salinity decrease by 2.5 in T1 and 5 in T2 (Miller et al., 2024a). Based on *in situ* photosynthetically  
190 active radiation (PAR) data collected in May 2021 with a LI-COR (model 192), irradiance was  
191 reduced from the control by a mean of 25% for T1, corresponding to the difference between the  
192 glacier-proximal inner region and the middle of the fjord, and 40% for T2, corresponding to the  
193 difference between the inner and outer parts of the fjord. To simulate the *in situ* light spectrum  
194 (Kai Bischof, pers. com.) and reach the irradiance matching the targeted treatments, green (RL244)  
195 and neutral Lee filters<sup>©</sup> (RL211; RL298) were placed on top of each mesocosm accordingly  
196 (Table 1). During the first week, all the mesocosms were maintained under *in situ* conditions of  
197 temperature, salinity, and irradiance. The light filters were then added to the mesocosms of T1 and  
198 T2 treatments on 2021-07-10, and all treatments gradually reached their targeted temperature and  
199 salinity conditions in six days. The experiment then lasted for six weeks.

200

### 201 **2.3 Tissue sampling**

202 Tissue samples were collected in the meristem (located directly above the stipe-frond junction on  
203 the frond) of ten individuals of *A. esculenta*, *L. digitata*, and *S. latissima* at the beginning of the  
204 experiment ( $t_0$ , 2021-07-03) and on the healthy organisms, namely complete organisms (frond,  
205 stipe, and holdfast) that exhibited a firm brown frond without signs of disease at the end ( $t_{final}$ ).  
206 pending determination of chlorophyll a (chl *a*, see section 2.4) and the carbon:nitrogen (C:N) ratio  
207 (see section 2.5). Samples were stored in aluminum foil at -20°C. Additional tissue samples were  
208 collected in the meristem of *S. latissima* and *H. nigripes* at  $t_{final}$  for gene expression analysis (n=8  
209 for each species, see section 2.7). These tissue samples were immediately flash-frozen in liquid  
210 nitrogen before being stored at -80°C.

211

### 212 **2.4 Chl *a* content**

213 Samples were blotted dry, weighed (wet weight), and ground with a glass pestle. Chl *a* was  
214 extracted in 90% aqueous acetone for 24 h in the dark at 4°C. After cold-centrifugation (0°C, 15  
215 min, 3000 rpm), the supernatants were transferred one at a time into a glass vial and the initial

Deleted: s

Deleted: in the Kongsfjorden

Deleted: and

Deleted: d

Deleted: under revision

Deleted: 0

Deleted: 3

Deleted:

Deleted: s

Formatted: Font: Bold

Formatted: Font: Bold

Deleted: 3

Deleted: 4

Deleted:

Deleted: and

Formatted: Font: Bold

Formatted: Font: Bold

Formatted: Font: Bold

Formatted: Font: Bold

Formatted: Font: Bold

229 fluorescence ( $F_0$ ) of chl *a* and pheophytin pigment were measured using a fluorometer (Turner  
 230 Design 10-AU Fluorometer; 667 nm). The  $F_a$  fluorescence (fluorescence after acidification) was  
 231 measured one minute after the addition of 10  $\mu$ l of 0.3 N HCl to transform chl *a* into pheophytin  
 232 pigment and subtract  $F_a$  from  $F_0$ . The chl *a* content was calculated using the formula of Lorenzen  
 233 (1967) but modified for determining chl *a* from mass of tissue rather than volume of seawater as:

$$Chl\ a\ (\mu g\ gFW^{-1}) = \frac{F_m}{(F_m - 1)} \frac{km(F_0 - F_a)}{m_{kelp}} \quad \text{Eq.1}$$

$$chl\ a\ (\mu g\ gFW^{-1}) = \frac{F}{(F_m - 1)}$$

234 where  $k$  is the calibration factor of pigment to fluorescence intensity [ $\mu$ g chl *a* mg solvent<sup>-1</sup>]  
 235 (instrument fluorescence unit<sup>-1</sup>),  $m$  is mass of acetone used for extraction (mg), and  $m_{kelp}$  is the  
 236 fresh weight of kelp (mg). Chl *a* content is expressed in  $\mu$ g per g of fresh weight ( $\mu$ g gFW<sup>-1</sup>).  
 237 No dilution factor was used as this was dry tissue mass.

### 241 2.5 C:N mass ratio

242 Samples were dried at 60°C for 48 h, weighed (dry weight), and their sizes adjusted to ensure that  
 243 they did not weigh more than 10 mg, the detection limits specific to the CHN analyzer  
 244 (PerkinElmer, Inc 2400). C and N contents are expressed in mg per g of dry weight (mg gDW<sup>-1</sup>).

### 246 2.6 Growth rate

247 Growth rate was determined using the hole puncture method of Parke (1948). Sporophytes were  
 248 punctured at  $t_0$  in the meristem section of each organism, 2 cm above the base of the frond. The  
 249 distance from the base of the frond to the hole was measured at  $t_{final}$ . The growth rate was calculated  
 250 as follows:

$$Growth\ rate\ (cm.\ d^{-1}) = \frac{dist_{final} - dist_0}{t_{final} - t_0} \quad \text{Eq.2}$$

254 with  $dist$  as the distance (in cm) from the base of the frond to the hole at time  $t$  (in days).

255 Weekly growth rates for selected individuals were determined at different time points during the  
 256 experiment for *S. latissima* (weeks 1 and 4) and *A. esculenta* (weeks 2 and 5). Results can be found  
 257 in the supplementary material (Fig. S2).

Deleted: i

Deleted: i

Formatted: Font: Italic

Deleted:

Formatted: Font: (Default) Times New Roman, 12 pt

Formatted: Centered

Deleted:

Formatted: Font: Italic

Formatted: Font: Italic

Formatted: Superscript

Formatted: Superscript

Formatted: Font: Italic

Formatted: Font: Italic

Formatted: Font: Italic, Subscript

Deleted: are

Formatted: Font: Italic

Formatted: Superscript

Deleted: diluton

Deleted: ). Chl *a* content are expressed in  $\mu$ g per g of fresh weight ( $\mu$ g gFW<sup>-1</sup>).

Deleted: ¶

Formatted: Font: Bold

Formatted: Font: Bold

Formatted: Font: Bold

Formatted: Font: Bold

Deleted:  $\mu$

Deleted:  $\mu$

Formatted: Font: Bold

Formatted: Font: Bold

Deleted: from the base of the

Deleted: frond

Deleted: stipe

Deleted: stipe

Formatted: Font: Italic

Formatted: Font: Italic

Deleted: with  $dist$ : distance (in cm) from the base of the stipe to the meristem at time  $t$  (in days)

Deleted: .

Deleted: as also

278

## 279 **2.7 Gene expression analysis**

280 *We chose to target two species for gene expression, *S. Latissima* and *H. nigripes*. *S. latissima**  
281 *was selected because it was the most abundant by biomass in the sampling area and appeared*  
282 *in robust physical health upon visual inspection at t<sub>final</sub>. *H. nigripes* was selected because it is*  
283 *an endemic Arctic species and, thus, a model comparison specimen.*

284 Total RNA extraction was conducted using the method described by Heinrich et al. (2012)  
285 which uses a CTAB extraction followed with a commercial Qiagen kit. The quantity and purity of  
286 the extracted RNA were evaluated using a Nanodrop ND-1000 Spectrophotometer  
287 (ThermoFisher), which measures RNA concentration at 260 nm and assesses purity by detecting  
288 the presence of other compounds such as DNA at 230 nm and proteins at 280 nm. The integrity of  
289 total RNA was determined by automated capillary electrophoresis using an Agilent 2100  
290 Bioanalyzer (Agilent Technologies). The cDNA libraries were constructed by poly(A) enrichment  
291 and sequenced on a NovaSeq 6000 instrument by the Genome Quebec platform. The 100 bp paired  
292 reads were clipped using default values of the Illumina software. The quality of raw sequences  
293 was checked using FastQC v.0.11.7  
294 (<https://www.bioinformatics.babraham.ac.uk/projects/fastqc/>). Sequences of low quality were  
295 trimmed using Trimmomatic v.0.39 (Bolger et al., 2014). For each species, a *de novo* transcriptome  
296 was constructed using the Trinity v.2.14.0 tool (Grabherr et al., 2011). The most homologous  
297 sequences were clustered using the CD-HIT-EST algorithm, part of the CD-HIT v.4.8.1 tool (Li  
298 and Godzik, 2006). To ensure the quality of the *de novo* transcriptomes, another transcriptome per  
299 species was generated using the rnaSPAdes v.3.14.1 (Bushmanova et al., 2019). Transcriptomes  
300 generated using rnaSPAdes and Trinity were compared using BUSCO v.5.4.3, transcriptomes  
301 generated with Trinity were retained due to lower duplicated sequences (Simão et al., 2015).  
302 Transcript quantification was performed by pseudo alignment using Kallisto v0.46.0, mapping  
303 RNA sequences to an index created from *de novo* transcriptomes (Bray et al., 2016). Exploration  
304 of differentially expressed genes (DEGs) was performed with the "DESeq2 v1.34.0" R package  
305 (Love et al., 2014). For each species, DEGs were obtained from the following comparisons: T1  
306 vs. C, T2 vs. C, T3 vs. C, T2 vs. T1, T3 vs. T1, and T3 vs. T2. Transcripts with an adjusted  $p <$   
307  $0.05$  and  $\log_2$  fold change (FC)  $> 2$  or  $< -2$  were considered significantly differentially expressed  
308 genes. Functional annotation of the genes was performed with eggNOG-mapper v2.1.10 against  
309 the eggNOG database v.5.0.2 (Huerta-Cepas et al., 2017 & 2019). To ensure they were properly  
310 annotated, annotation was also performed with TransDecoder v5.5.0 to predict coding sequences  
311 (Haas and Papanicoualo, 2015), which were aligned against a Pfam profile database v35.0 (Mistry

Formatted: Font: Bold

Formatted: Font: Italic

Formatted: Font: Italic

Formatted: Font: Italic

Formatted: Normal, Right: 0"

Formatted: Font: Italic

Formatted: Font: Bold

Formatted: Indent: First line: 0.5"

Deleted: with



313 et al., 2021) using the HMMER v3.3 alignment tool (Finn et al., 2011). Gene Ontology (Gene  
314 Ontology Consortium, 2015) terms were then retrieved from the pfam2go database  
315 (<https://pypi.org/project/pfam2go/>) and functional enrichment was performed with Ontologizer  
316 v2.1 to obtain statistically significant GOs from the DEGs of each comparison performed  
317 previously (Bauer et al., 2008). Functional enrichment results were summarized as tree plots and  
318 scatter plots using REVIGO v1.8.1 (Supek et al., 2011). Investigation of the specific functions of  
319 DEGs was carried out by manually checking the involvement of Pfam domains and EggNOG  
320 annotations on the SMART database v9.0 (Letunic et al., 2021). Some DEGs whose annotation  
321 was questionable (i.e. not referring to plant genomes such as gene collagen) were removed, as well  
322 as those whose annotation was not precise enough to be classified. DEGs were then classified into  
323 different categories: cytoskeleton, genetic transcription/translation, metabolism, signaling,  
324 transport, stress (heat stress and oxydo-reduction processes), and energy production (respiration  
325 and photorespiration). A part of DEGs (73.2% in *S. latissima* and 82.3% in *H. nigripes*) were  
326 trimmed as they lacked functional annotation. Tools and parameters are summarized in Table S1.

Deleted:

## 328 **2.8 Statistics**

Formatted: Font: Bold

329 Rosner's generalized Extreme Studentized Deviation (ESD) test was used to detect the outliers  
330 using the function `rosnerTest` of the R package "`EnvStats`" (Millard, 2013). Out of a total of 165  
331 individual chl *a* measurements, when combining all species and conditions, eleven were identified  
332 as outliers and removed. After the removal of the outliers, the normal distribution of the data was  
333 verified with a Shapiro-Wilk test using the function `shapiro.test` from the "`stats`" R package (R  
334 Core Team, 2013;  $p > 0.105$ ). No outliers were identified in the C:N and growth rate data and  
335 normality was verified ( $p > 0.089$ ).

Formatted: Font: Bold

336 Chl *a* content and C:N were analyzed using a linear mixed model with a hierarchical  
337 structure (HLM) to evaluate treatment effects by species. The model was fitted using the function  
338 `lmer` in the R package "`lme4`" (Bates et al., 2015). The fixed factors for the model were treatment  
339 and species, while mesocosm was a random factor. For growth rate measurements, a generalized  
340 linear mixed model (GLMM) with a Gaussian distribution was preferred - based on an Akaike  
341 information criterion - to test for the effects of the species, treatment, and mesocosm replica.

Formatted: Indent: First line: 0.5"

## 342 **3. Results**

### 343 **3.1 Experimental conditions**

Formatted: Font: Bold

344 The median temperature value in the control treatment was 5.3°C during the experimental period  
345 (2021-07-16 to 2021-08-28) calculated based on the mean value across replicates (Fig. 2, Table

Formatted: Font: Bold



347 1). The median salinity was 33.8 and the median daily PAR was 47.8  $\mu\text{mol photons m}^{-2} \text{ s}^{-1}$ . In  
348 treatment T1, the median temperature, salinity, and PAR were 8.9°C, 31, and 36.1  $\mu\text{mol photons}$   
349  $\text{m}^{-2} \text{ s}^{-1}$ , respectively. For treatments T2 and T3, the median temperature was elevated to 10.8°C. In  
350 T2, median salinity and PAR were decreased to 28.5, and 31.4  $\mu\text{mol photons m}^{-2} \text{ s}^{-1}$ .

351

### 352 **3.2 Chl *a* content**

353 The factors species and treatment were found as significant predictors, including their interaction  
354 when assessing differences in measured chl *a* content at  $t_0$  and  $t_{\text{final}}$  ( $p < 0.001$ ; Table S2). For *A.*  
355 *esculenta*, the concentration of chl *a* decreased significantly between  $t_0$  and the control at  $t_{\text{final}}$  ( $p <$   
356 0.01, Fig. 3, Table S3). Values in the T2 treatment were also significantly higher than the control,  
357 T1, and T3 treatments (all  $p$  were  $< 0.01$ ). Values in the control, T1, and T3 treatments were not  
358 statistically different from each other ( $p > 0.92$ ). Similarly to *A. esculenta*, chl *a* content of *S.*  
359 *latissima* significantly decreased between  $t_0$  and  $t_{\text{final}}$  ( $p = 0.02$ ) for the control, but were not  
360 significantly impacted by the treatments ( $p > 0.99$ ). The chl *a* content of *L. digitata* was not  
361 significantly impacted by time and treatments ( $p > 0.99$ ).

362

### 363 **3.3 C:N ratio**

364 The statistical significance of predictor variables species and treatment for C:N, carbon content,  
365 and N content were significantly different for species and treatment ( $p < 0.001$ ; Table S4), with  
366 the exception of treatment as a non-significant predictor for carbon content. There were no  
367 significant interactions between species and treatment. The pairwise comparisons determined that  
368 for *S. latissima*, C:N ratios at  $t_0$  ranged from 24.5 up to 37.1 (Fig. 4). No statistical difference was  
369 found between  $t_0$ , the control, T1, and T3 treatment at  $t_{\text{final}}$  ( $p > 0.93$ , Tables S4, S5). In contrast,  
370 C:N ratios of individuals in the T2 treatment were significantly lower than at  $t_0$ , ranging from 15.2  
371 to 29.5 (Fig. 4A,  $p = 0.045$ ). Although carbon content showed no significant difference across  
372 treatments and time (Fig. 4B,  $p = 1$ ), there was a notable increase in nitrogen content in the T2  
373 treatment compared to  $t_0$ , but it was not statistically significant (Fig. 4C,  $p = 0.06$ ). The C:N ratios,  
374 carbon, and nitrogen contents of *A. esculenta* and *L. digitata* were not significantly impacted by  
375 the treatments ( $p > 0.32$ ).

376

### 377 **3.4 Growth rate**

378 The growth rates of *A. esculenta*, *L. digitata*, and *S. latissima* were not significantly impacted by  
379 the treatments (Fig. 5,  $p = 1$ , Tables S6, S7). They ranged from 0 to 0.037  $\text{cm d}^{-1}$  for *A. esculenta*,

Formatted: Font: Bold

Formatted: Font: Bold

Formatted: Font: Bold

Formatted: Font: Bold

Commented [1]: It look like it according to table S3

Formatted: Font: Italic

Formatted: Subscript

Deleted: s S2,

Deleted: different from

Deleted: ¶

Deleted: ¶

Deleted:

Formatted: Font: Bold

Formatted: Font: Bold

Formatted: Font: Italic

Deleted: For

Deleted: ¶

Formatted: Font: Bold

Formatted: Font: Bold

387 0.007 to 0.046 cm d<sup>-1</sup> for *L. digitata*, and 0.040 up to 0.509 cm d<sup>-1</sup> for *S. latissima*. The growth rate  
388 of *S. latissima* was significantly higher than for the two other species for each treatment ( $p < 0.01$ ).  
389 The growth rate of *A. esculenta* significantly decreased between week 2 and week 6 ( $p < 0.01$ , Fig.  
390 S1A) over time in the control. For *S. latissima*, **significant differences in growth over time were**  
391 **only found in the T3 treatment**, ( $p=0.02$ , Fig. S1B). No intermediate measurements of *L. digitata*  
392 growth rate were taken.

Deleted: no significant differences were found over time in the C, T1 and T2, except in the T3 treatment

393

### 394 **3.5 Gene expression analysis**

395 **Principal component analysis of global gene expression revealed** a clear contrast between the  
396 control and the different treatments for both *S. latissima* and *H. nigripes* (Fig. S2). The number of  
397 total differentially expressed genes (DEGs, i.e. genes that are either up- or down-regulated when  
398 comparing the different treatments to the control) were close between *S. latissima* (831 including  
399 225 classified; **i.e. functionally annotated**) and *H. nigripes* (815 including 144 classified, Fig. 6A)  
400 and mostly down-regulated for both species (84 and 65% respectively). For *H. nigripes*, the  
401 majority of overlapping DEGs were found between treatments T1 and T2 (Fig. 6A). Conversely,  
402 for *S. latissima*, the highest number of overlapping DEGs was observed between treatments T1  
403 and T3. In both species, no overlapping genes were identified when comparing the DEGs between  
404 treatment pairs T1 vs. T2 and T2 vs. T3 (Fig. 6B).

Formatted: Font: Bold

Formatted: Font: Bold

Deleted: The analysis of gene expression revealed

405 The highest number of DEGs were exhibited in the transcription/translation and  
406 metabolism classes in *H. nigripes* (Fig. 7A) and in the transcription/translation and cytoskeleton  
407 classes for *S. latissima* (Fig. 7B). For this last species, the T3 treatments caused the highest number  
408 of down-regulated genes (607 including 152 classified) with 60% belonging to the three classes  
409 mentioned above, followed by T1 (314 including 47 classified) and T2 (247 including 56  
410 classified; Fig. 6 and 7). For *H. nigripes*, 600 genes were observed to be regulated in T2 including  
411 458 genes down-regulated. **A substantial portion of the classified down-regulated genes belongs**  
412 **to the transcription/translation and metabolism class (64%), followed by an approximately equal**  
413 **proportion of genes associated with photorespiration (13%), stress (11%), and transport (8%) and**  
414 **lesser proportions of genes associated with other functions. Genes belonging to the**  
415 **photorespiration/energy production class, involved either in the photosynthesis or respiration**  
416 **process, were found to be down-regulated in *H. nigripes* in T2 and in *S. latissima* in T2 and T3.**  
417 **Stress genes were down-regulated in all treatments for both species. [The list of DEGs is available](#)**  
418 **[in the Supplementary material.](#)**

Formatted: Indent: First line: 0.5"

Deleted: ing

Deleted: ing

Deleted:

Deleted: ¶

419

#### 427 4. Discussion

428 The analysis of gene expression combined with the investigated physiological parameters show  
429 the ability of Arctic kelps to acclimate to a range of environmental conditions. Indeed, no **negative**,  
430 impacts of the treatments **were** recorded, even according to the highest emission scenarios (SSP5-  
431 8.5). This observation confirms that these species, originating from lower latitudes, could thrive  
432 in a warmer Arctic. **This corroborates the findings of Miller et al. (2024b) which shows a tolerant**  
433 **community level response to the same experimental conditions. Further, this also refutes our**  
434 hypothesis that the combined effects of high temperature, low salinity, and low irradiance will  
435 necessarily have a negative impact on their physiology.

436

##### 437 4.1 Chl *a* content

438 We hypothesized that different species might have different responses to a changing environment.  
439 The chl *a* content of both *A. esculenta* and *S. latissima* in the meristem part of the frond showed a  
440 significant decrease from  $t_0$  to  $t_{\text{final}}$  in the control (-45% and -70% respectively). The same trend  
441 was observed in *L. digitata* although this is not significant due to the low number of measurements  
442 (-57%,  $n=3$  at  $t_{\text{final}}$ ). The high level of chl *a* measured in early summer matches the anticipation of  
443 ice melting and the following increase in turbidity (Aguilera et al., 2002). Decreasing chl *a* content  
444 between June and August has already been reported *in situ* in Kongsfjorden for *S. latissima*  
445 (Aguilera et al., 2002) with the end of the growth period (Berge et al., 2020).

446 In contrast to what was observed in the control as well as in the T1 and T3 treatments, for  
447 *A. esculenta*, the chl *a* content in the warm, less saline, and **lower irradiance treatment (T2)**  
448 remained as high as it was at  $t_0$ . The decrease in irradiance in this treatment may explain the  
449 persistence of elevated chl *a* levels. PAR is often negatively correlated with chl *a* content as higher  
450 chl *a* can help maintain elevated photosynthetic rates under reduced PAR (e.g. McWilliam and  
451 Naylor, 1967; Zhang et al., 2014). Bartsch et al. (2016) showed that the genus *Alaria* was more  
452 abundant than *Laminaria* and *Saccharina* between 10 and 15 m depth. Despite a decrease in  
453 irradiance caused by glacial and terrestrial runoff, *A. esculenta* is the only species that extended  
454 its maximum depth (from 15 to 18 m between 1994/96 to 2014; Bartsch et al., 2016). This shift  
455 could be explained by an **existing adaptation** to low PAR (Niedzwiedz and Bischof, 2023), giving  
456 this species a competitive advantage at greater depth. Our findings shed light on the adaptive  
457 responses of *A. esculenta* to low light, and seemingly tolerance to low salinity and warming,  
458 suggesting that this species will most likely be able to withstand future coastal environmental  
459 conditions in the Arctic.

Deleted: negatively

Deleted: as

Deleted: s

Deleted: Miller et al.,

Deleted: T

Formatted: Font: Bold

Formatted: Font: Bold

Formatted: Font: Bold

Formatted: Font: Bold

Formatted: Indent: First line: 0.5"

Deleted: with

Deleted: effective short-term acclimation

467 The chl *a* content of *L. digitata* and *S. latissima* was also not affected by the treatments.  
468 This is in agreement with the study of Diehl and Bischof (2021) where temperature (up to 10°C),  
469 combined with low salinity (down to 25) did not affect the chl *a* content of *S. latissima*. However,  
470 their growth rate in low light conditions remained similar to the other treatments. Other  
471 physiological processes such as photosynthetic efficiency, or resource allocation, might have been  
472 altered to maintain growth rates similar to the control.

Deleted: f

Deleted: chl *a* of

Formatted: Font: Italic

#### 473 474 **4.2 C:N ratio**

Formatted: Font: Bold

475 The C:N ratio of *S. latissima* was significantly lower in the T2 treatment compared to  $t_0$ . The  
476 decrease in C:N ratio seems driven by an increase in nitrogen uptake. Benthic marine macroalgae  
477 and seagrasses from temperate and tropical regions have a mean C:N ratio of 22 (Atkinson and  
478 Smith, 1983). In northern Norway, Liesner et al. (2020) reported a C:N ratio of 21 for *L. digitata*  
479 which is consistent with our measurements for this species as well as for *A. esculenta*, all  
480 treatments and sampling times combined. However, *S. latissima* exhibited higher ratios with a  
481 mean of  $29.7 \pm 5.5$  ( $t_0$  and  $t_{\text{final}}$  of the control, T1 and T3 combined), which would suggest nitrogen  
482 limitation. While algae in the T2 treatment showed a higher nitrogen content, which is an essential  
483 nutrient playing a central role in photosynthesis and protein biosynthesis, the growth rate remained  
484 similar to the other treatments. Gordillo et al. (2002) showed higher nitrogen uptake at lower  
485 salinity (50% vs. 100% seawater) in *Fucus serratus* that was explained by increased N metabolism.  
486 Thus, the higher nitrogen content found here in the low saline T2 treatment (salinity down to 28)  
487 could have resulted from increased N metabolism. Indeed, the increase in nitrogen concentration  
488 in the macroalgae can induce an increase in the activity of nitrate reductase (Korb and Gerard,  
489 2000). This enzyme catalyzes the first step in the reduction of nitrate to organic forms and protein  
490 synthesis. In fact, nitrate concentration in water was higher in the T2 treatment ( $1.68 \pm 0.8 \mu\text{M/L}$ )  
491 than in the control ( $0.87 \pm 0.9 \mu\text{M/L}$ , data not shown) during the duration of the experiment. Arctic  
492 coastal waters are known to be nitrate-limited (Santos-Garcia et al., 2022). The influx of fresh and  
493 potentially more nitrate-rich waters may have induced an increase in the N metabolism of *S.*  
494 *latissima* which was nitrogen limited. Higher nutrient input from land through coastal erosion and  
495 permafrost thawing may benefit this species in various processes such as photosynthesis,  
496 biosynthesis, immunity and/or molecule transport (Campbell, 1988; Meyer et al., 2005).

Deleted: northern

Deleted: the

Deleted: treatment

#### 497 498 **4.3 Growth rate**

Formatted: Font: Bold

499 We also hypothesized that warming may enhance the growth rate of kelp. None of the growth rates  
500 of the three study species were affected by the different treatments over the total duration of the

506 experiment. In contrast, previous studies observed an increase of the growth rate of *S. latissima*  
507 when exposed to warmer conditions (8–10°C vs. 0–4°C under replete irradiance; Iníguez et al.,  
508 2016; Olischläger et al., 2017; Li et al., 2020; Diehl and Bischof, 2021). This discrepancy with our  
509 results can be explained by the duration of the experiment (7 to 18 days in previous studies vs 6  
510 weeks here), the study period, and the irradiance. Our study was performed at the end of the peak  
511 growth (mid-May to July) and after, while other studies were performed in early July or used  
512 sporophytes raised from gametophyte cultures. The growth rate of *A. esculenta* significantly  
513 decreased over time in the control, indicating the gradual end of the growth peak, with many of  
514 the kelp starting to senesce (Fig. S1A). For *S. latissima*, no significant differences were found over  
515 time in the control, indicating that the experiment started after the growth peak (Fig. S1B; Berge et  
516 al., 2020). In the T3 treatment only, growth was stimulated only during the first four weeks of the  
517 experiment, suggesting that warming may have prolonged the growth rate of *S. latissima* after the  
518 end of the peak growth period. Further studies may focus on this aspect. The T2 treatment did not  
519 induce a growth stimulation suggesting a negative effect of salinity and/or low irradiance.

Deleted: -

Deleted: -

Deleted: f

Deleted: C

#### 520 521 **4.4 Gene expression**

Formatted: Font: Bold

522 Both *H. nigripes* and *S. latissima* exhibited different gene expressions in the control compared  
523 to the treatments. The fact that treatments are not clustered separately from each other but are  
524 grouped together against the control suggests that the common factor among them, which is  
525 the increase in temperature, might be the key influencing factor.

526 Interestingly, and as we hypothesized, the response to these treatments differed between  
527 the two species. The analysis of DEGs shows that the low salinity and irradiance treatment (T2)  
528 had a higher impact on the number of genes regulated in *H. nigripes* while warming alone (T3)  
529 had a higher impact on genes regulation on *S. latissima*. Since no phenotypic response was  
530 observed for *S. latissima* in T3, this suggests that the observed down-regulation might be an  
531 acclimation mechanism enabling the organism to maintain its main processes. Other  
532 parameters could be measured to validate this hypothesis (lipid content, photosynthesis rates,  
533 accessory pigment concentrations, etc). Li et al., (2020) found a regulation of genes involved  
534 in reducing the osmotic pressure under low-salinity stress in *S. latissima* (salinity of 20 vs. 30).  
535 We did not observe such results with this species nor with *H. nigripes*, most likely because the  
536 reduction in salinity was much smaller in our experiment (up to -5 here vs -10 in Li et al.,  
537 2020). However, for both species, the T2 treatment induced a down-regulation of  
538 photorespiratory genes. This is consistent with previous observations in *S. latissima* (Monteiro  
539 et al., 2019). Under stressful conditions like hyposalinity, kelp may prioritize acclimatization

Formatted: Indent: First line: 0.5"

Deleted: to

Deleted: reduce

546 and survival strategies over photosynthesis. Photosynthesis was however not measured during  
547 the experiment to validate this hypothesis.

548 Finally, we noticed a down-regulation, rather than the expected up-regulation, of heat-shock  
549 proteins (HSP), despite their typical induction under abiotic stress (Sørensen et al., 2003). The  
550 regulation of HSP in response to salinity variations occurs to a lesser degree compared to its  
551 response to temperature changes (Monteiro et al., 2019). Considering that these species  
552 originate from lower latitudes, their current exposure to the low temperatures in the Arctic  
553 might induce stress, while future warmer waters may reduce it. *For example, the increased  
554 growth rate observed for *S. latissima* could likely be a response to the increased activity of  
555 RuBisCO inducing faster energy production, and resulting in the observed N-limitation.  
556 Further, the down-regulation of stress responses may indeed be a function of reduced energy  
557 input to maintain homeostasis in warmer waters. It is important to note, however, that the high  
558 temperature exposure treatment approaches the thermal optimum for *S. latissima* (Andersen et  
559 al., 2013), and may likely be close to the peak of enzymatic activity. Thus, increased warming  
560 beyond what was tested in this experiment may begin to induce a stress response and the  
561 subsequent down-regulation of enzymatic activity.*

#### 563 **4.5 Future prospects of *Alaria esculenta*, *Saccharina latissima*, *Laminaria digitata*, and 564 *Hedophyllum nigripes* in the Arctic**

565 Our findings support the hypothesis that *A. esculenta* is more likely to be resilient to future changes  
566 in irradiance than other kelp species. In particular, our results reveal its competitive advantage at  
567 depth, through its *increased chl *a* content*. However, no discernible positive impact was observed  
568 on its growth rate in low light conditions. This impact may be more evident earlier in the season,  
569 during the peak growth. *A. esculenta* seems resilient to increasing glacier and river runoff,  
570 becoming more dominant in low-light environments such as greater depths (Bartsch et al., 2016).  
571 The dominance of a single kelp species in specific regions may carry ecological consequences, as  
572 reduced diversity threatens ecosystem resilience (Loreau et al., 2001).

573 For *L. digitata*, our results demonstrate neither negative nor positive effects of warming,  
574 low salinity, and low irradiance. Franke et al. (2021) also found no effect of a 5°C warming on the  
575 growth rate of this species (control: 5°C, warming: 10°C). However, in our study confusion with  
576 *H. nigripes* at  $t_0$  has split the data, making the analysis less robust. Indeed, the individuals could  
577 only be identified at the end of the experiment, after cutting the stipe. This led to the removal of  
578 16 individuals from the analysis. The slight decrease in the content of chl *a* over time, as observed  
579 for the other two species in the study, could not be confirmed statistically. Bartsch et al. (2016)

Formatted: Font: Italic

Deleted: inducing

Deleted: production

Deleted: down-regulation

Deleted: energy

Deleted: homeostasis

Deleted: is close to

Deleted: optimum

Deleted:

Formatted: Font: Italic

Deleted: (REF)

Deleted: likely

Formatted: Font: (Default) Times New Roman, 12 pt

Deleted: experiment

Formatted: Font: Bold

Deleted: high content

Deleted: in chl *a*

Deleted: N

Deleted: of its higher chlorophyll *a* content

Formatted: Font: Italic

Formatted: Indent: First line: 0.5"

595 found that *L. digitata* was the only species that experienced a significant increase in biomass  
596 between 1994/1996 and 2014 on the entire transect they studied (from 0 to 15 m depth). Current  
597 and future conditions in the short term seem optimal for this species. Germination of *L. digitata* is  
598 enhanced at 9°C compared to 5°C and 15°C (Zacher et al., 2016, 2019) and its growth rate is higher  
599 at 15°C compared to 5°C and 10°C (Franke et al., 2021). Although warming alone may be  
600 beneficial to this species, its combined effects with other environmental factors **as well as biotic**  
601 **interactions (e.g. Zacher et al., 2019)** might be detrimental once a certain threshold is reached.  
602 Muller et al. (2008) found no difference in the germination rate between 7°C and 12°C, but showed  
603 that germination under UV of type A and B decreased down to less than 30% at 12°C compared  
604 to almost 80% at 7°C. **We acknowledge that the low sample size for *L. digitata* could obscure the**  
605 **observation of potential negative impacts, and, thus, future studies should aim to increase study**  
606 **sample sizes and the temporal variability of *L. digitata* resilience to future climate scenarios.**  
607 **Unfortunately, this would have been logistically challenging given our experimental setup.**

608 *S. latissima* is widely studied throughout the northern hemisphere. In the Arctic  
609 specifically, several studies indicate that future conditions may favor the expansion of this species.  
610 This is supported by findings of enhanced germination with temperatures up to 12°C (Muller et  
611 al., 2008) and mitigation of the negative effects of UV radiation at high temperatures (12°C;  
612 Heinrich et al., 2015). Our results reveal that *S. latissima* may benefit from increasing N input  
613 from coastal erosion and permafrost thawing that could enhance immunity, photosynthesis,  
614 biosynthesis and/or molecule transport, although this was not measured in this study. *S. latissima*  
615 exhibits a high degree of polymorphism, acclimation, and genetic diversity across populations  
616 (Bartsch et al., 2008; Guzinski et al., 2016). For example, its growth shows a high phenotypic  
617 plasticity that appears to be constrained within specific seasonal **growth patterns in accordance**  
618 **with their environment of origin** (Spurkland and Iken, 2011). In the Canadian Arctic, Goldsmit  
619 et al. (2021) found that suitable habitat of this species may gain 64,000 km<sup>2</sup> by 2050, most of this  
620 new area being in the northernmost reaches, where temperature is rising and sea ice is receding.  
621 Bartsch et al. (2016) found a 30-time increase in its biomass between 1994/1996 in 2014 at 2.5 m  
622 depth at Hansneset (Kongsfjorden, Svalbard, Norway). *S. latissima* will most likely benefit from  
623 future conditions although the capacity and time of dispersal, as well as competition with other  
624 species, predation, and extreme events must be considered for population projections.

625 So far, *A. esculenta*, *L. digitata*, and *S. latissima* have adapted successfully to the shifting  
626 Arctic environment and our results suggest that they might thrive in the conditions expected for  
627 2100. In the short term, these species may well continue to spread in this region. Regarding *H.*  
628 *nigripes*, Franke et al. (2021) suggested a true Arctic affinity with a sporophyte growth optimum

Deleted: ,

Deleted: acknowledge

Formatted: Font: Italic

Deleted: possibly

Deleted: resilience

Formatted: Font: Italic

Deleted: Unfortunately

Deleted: logistically

Deleted: challenging

Deleted: ta

Deleted: ,

Deleted: a



639 of 10°C. By 2100, this species might continue to thrive in the Arctic, as evidenced by our gene  
640 expression analysis, which suggests efficient acclimation with less stress under future scenarios.

Deleted: tiza

641 Kelp species will, however, face more competition, grazing, and extreme events such as high  
642 sedimentation rate, ice-scouring, and marine heatwaves (Hu et al., 2020). Around Tromsø  
643 (Norway), the massive spread of sea urchins may have caused the ecosystem to collapse into a  
644 barren state (Sivertsen et al., 1997). Moreover, with warming, the frequency and intensity of  
645 marine heatwaves will increase which could have important consequences on marine species of  
646 Arctic flora and fauna. These potential effects of climate change should be taken into account to  
647 better assess the future of Arctic kelp communities. It therefore appears essential to continue to  
648 study these communities in order to predict and anticipate future changes and impacts on fisheries,  
649 local and indigenous people, and on a global scale.

Deleted: e new

## 650 **Acknowledgment**

651 We are grateful to the staff of the Alfred Wegener Institute (AWI), Institut polaire français Paul  
652 Emile Victor (IPEV), and Kings bay for field assistance. We thank Cátia Monteiro for her advice  
653 on RNA extraction and Erwan Corre for his expertise and guidance to process transcriptomic data.  
654 Thanks are also due to Inka Bartsch, Kai Bischof, and Simon Jungblut for their input, which  
655 improved the design and interpretation of this study, and Nathalie Leblond for her help with the  
656 CHN analysis. This study was conducted in the frame of the project FACE-IT (The Future of  
657 Arctic Coastal Ecosystems – Identifying Transitions in Fjord Systems and Adjacent Coastal  
658 Areas). FACE-IT has received funding from the European Union’s Horizon 2020 research and  
659 innovation programme under grant agreement No 869154. We also acknowledge the support of  
660 IPEV (project ARCTOS 1248) and the Prince Albert II of Monaco Foundation (project ORCA  
661 n°3051).

## 662 **Author contributions**

663 AL, CM, SC, PU, SA, RS, JPG, and FG were involved in the fieldwork. AL, CM, SC, JPG, and  
664 FG designed the study. SC, PU, and FG designed the system. The experiment was conducted by  
665 AL, CM, SC, SA, RS, JPG, and FG. AL and CM performed measurements of the chl *a* content.  
666 AL performed the C:N ratio measurement and the RNA extractions. MM processed transcriptomic  
667 data. AL analyzed the data and wrote the first draft of the manuscript, which was then finalized by  
668 all co-authors.

Deleted:

## 670 **Code and data availability**

Formatted: Font: Bold

Formatted: Font: Bold

Formatted: Font: Bold

674 [The code used to carry out the majority of bio-info processes can be found at:](#)  
675 <https://github.com/MarcMeynadier/SaccharinaHedophyllumTranscriptomic>. All data (except for  
676 [gene expression](https://doi.pangaea.de/10.1594/PANGAEA.971349)) are available at <https://doi.pangaea.de/10.1594/PANGAEA.971349>.

677

## 678 References

679 Aguilera, J., Bischof, K., Karsten, U., Hanelt, D., Wiencke, C., 2002. Seasonal variation in  
680 ecophysiological patterns in macroalgae from an Arctic fjord. II. Pigment accumulation and  
681 biochemical defence systems against high light stress. *Marine Biology* 140, 1087–1095.  
682 <https://doi.org/10.1007/s00227-002-0792-y>

683 Ahmed, R., Prowse, T., Dibike, Y., Bonsal, B., O’Neil, H., 2020. Recent trends in freshwater  
684 influx to the Arctic Ocean from four major Arctic-draining rivers. *Water* 12, 1189.

685 [Andersen, G. S., Pedersen, M. F., and Nielsen, S. L., 2013. Temperature acclimation and heat](#)  
686 [tolerance of photosynthesis in Norwegian \*Saccharina latissima\* \(Laminariales, Phaeophyceae\).](#)  
687 [Journal of Phycology, 49, 689–700. <https://doi.org/10.1111/jpy.12077>](#)

Formatted: Font: (Default) Times New Roman

Formatted: Font: (Default) Times New Roman

Formatted: Font: (Default) Times New Roman, Italic

Formatted: Font: (Default) Times New Roman

Formatted: Font: (Default) Times New Roman

688 Atkinson, M.J., Smith, S.V., 1983. C:N:P ratios of benthic marine plants. *Limnology and*  
689 *Oceanography* 28, 568–574. <https://doi.org/10.4319/lo.1983.28.3.0568>

690 Bartsch, I., Paar, M., Fredriksen, S., Schwanitz, M., Daniel, C., Hop, H., Wiencke, C., 2016.  
691 Changes in kelp forest biomass and depth distribution in Kongsfjorden, Svalbard, between 1996–  
692 1998 and 2012–2014 reflect Arctic warming. *Polar Biology* 39, 2021–2036.

693 Bartsch, I., Wiencke, C., Bischof, K., Buchholz, C.M., Buck, B.H., Eggert, A., Feuerpfeil, P.,  
694 Hanelt, D., Jacobsen, S., Karez, R., Karsten, U., Molis, M., Roleda, M.Y., Schubert, H.,  
695 Schumann, R., Valentin, K., Weinberger, F., Wiese, J., 2008. The genus *Laminaria* sensu lato:  
696 recent insights and developments. *European Journal of Phycology* 43, 1–86.  
697 <https://doi.org/10.1080/09670260701711376>

Deleted:

698 Bates, D., Mächler, M., Bolker, B., Walker, S., 2015. Fitting linear mixed-effects models using  
699 lme4. *Journal of Statistical Software* 67. <https://doi.org/10.18637/jss.v067.i01>

700 Bauer, S., Grossmann, S., Vingron, M., Robinson, P.N., 2008. Ontologizer 2.0—a multifunctional  
701 tool for GO term enrichment analysis and data exploration. *Bioinformatics* 24, 1650–1651.

702 Berge, J., Johnsen, G., Cohen, J., 2020. Polar night marine ecology. *Advances in Polar Ecology* 4.

703 Bischof, K., Hanelt, D., Wiencke, C., 1999. Acclimation of maximal quantum yield of  
704 photosynthesis in the brown alga *Alaria esculenta* under high light and UV radiation. *Plant*  
705 *Biology* 1, 435–444. <https://doi.org/10.1111/j.1438-8677.1999.tb00726.x>

706 Bolger, A.M., Lohse, M., Usadel, B., 2014. Trimmomatic: a flexible trimmer for Illumina  
707 sequence data. *Bioinformatics* 30, 2114–2120.

709 [Bolton, J. J. and Lüning, K., 1982. Optimal growth and maximal survival temperatures of Atlantic](#)  
710 [Laminaria species \(Phaeophyta\) in culture, Mar. Biol., 66, 89–94,](#)  
711 <https://doi.org/10.1007/BF00397259>

Formatted: Font: (Default) Times New Roman

Formatted: Font: (Default) Times New Roman

Formatted: Font: (Default) Times New Roman

712 Bray, N.L., Pimentel, H., Melsted, P., Pachter, L., 2016. Near-optimal probabilistic RNA-seq  
713 quantification. Nature biotechnology 34, 525–527.

714 Bushmanova, E., Antipov, D., Lapidus, A., Prjibelski, A.D., 2019. rnaSPAdes: a de novo  
715 transcriptome assembler and its application to RNA-Seq data. GigaScience 8, giz100.

716 Campbell, W.H., 1988. Nitrate reductase and its role in nitrate assimilation in plants. Physiologia  
717 Plantarum 74, 214–219. <https://doi.org/10.1111/j.1399-3054.1988.tb04965.x>

718 Dankworth, M., Heinrich, S., Fredriksen, S., Bartsch, I., 2020. DNA barcoding and mucilage ducts  
719 in the stipe reveal the presence of *Hedophyllum nigripes* (Laminariales, Phaeophyceae) in  
720 Kongsfjorden (Spitsbergen). Journal of Phycology 56, 1245–1254.  
721 <https://doi.org/10.1111/jpy.13012>

722 Diehl, N., Bischof, K., 2021. Coping with a changing Arctic: mechanisms of acclimation in the  
723 brown seaweed *Saccharina latissima* from Spitsbergen. Marine Ecology Progress Series 657, 43–  
724 57. <https://doi.org/10.3354/meps13532>

Formatted: Default Paragraph Font, Font: (Default) Arial, 11 pt

725 [Diehl, N., Roleda, M. Y., Bartsch, I., Karsten, U., and Bischof, K., 2021. Summer Heatwave](#)  
726 [Impacts on the European Kelp \*Saccharina latissima\* Across Its Latitudinal Distribution](#)  
727 [Gradient. Front. Mar. Sci., 8, https://doi.org/10.3389/fmars.2021.695821](#)

Formatted: Font: (Default) Times New Roman

Formatted: Font: (Default) Times New Roman

Formatted: Left, Right: 0", Space After: 12 pt, Line spacing: single, Don't adjust space between Latin and Asian text, Don't adjust space between Asian text and numbers

Formatted: Font: (Default) Times New Roman, Italic

Formatted: Font: (Default) Times New Roman

Formatted: Font:

728 Eggert, A., 2012. Seaweed Responses to Temperature, in: Wiencke, C., Bischof, K. (Eds.),  
729 Seaweed biology: novel insights into ecophysiology, Ecology and Utilization, Ecological Studies.  
730 Springer, Berlin, Heidelberg, pp. 47–66. [https://doi.org/10.1007/978-3-642-28451-9\\_3](https://doi.org/10.1007/978-3-642-28451-9_3)

731 Filbee-Dexter, K., Wernberg, T., Fredriksen, S., Norderhaug, K.M., Pedersen, M.F., 2019. Arctic  
732 kelp forests: diversity, resilience and future. Global and Planetary Change 172, 1–14.  
733 <https://doi.org/10.1016/j.gloplacha.2018.09.005>

734 Finn, R.D., Clements, J., Eddy, S.R., 2011. HMMER web server: interactive sequence similarity  
735 searching. Nucleic Acids Research 39, W29–W37. <https://doi.org/10.1093/nar/gkr367>

736 Franke, K., Liesner, D., Heesch, S., Bartsch, I., 2021. Looks can be deceiving: contrasting  
737 temperature characteristics of two morphologically similar kelp species co-occurring in the Arctic.  
738 Botanica Marina 64, 163–175. <https://doi.org/10.1515/bot-2021-0014>

739 Gene Ontology Consortium, 2015. Gene ontology consortium: going forward. Nucleic acids  
740 research 43, D1049–D1056.

741 Goldsmit, J., Schlegel, R.W., Filbee-Dexter, K., MacGregor, K.A., Johnson, L.E., Mundy, C.J.,  
742 Savoie, A.M., McKindsey, C.W., Howland, K.L., Archambault, P., 2021. Kelp in the eastern  
743 Canadian Arctic: current and future predictions of habitat suitability and cover. Frontiers in Marine  
744 Science 18, 742209. <https://doi.org/10.3389/fmars.2021.742209>

745 Gordillo, F., Dring, M., Savidge, G., 2002. Nitrate and phosphate uptake characteristics of three  
746 species of brown algae cultured at low salinity. *Marine Ecology Progress Series* 234, 111–118.  
747 <https://doi.org/10.3354/meps234111>

748 Grabherr, M.G., Haas, B.J., Yassour, M., Levin, J.Z., Thompson, D.A., Amit, I., Adiconis, X.,  
749 Fan, L., Raychowdhury, R., Zeng, Q., 2011. Full-length transcriptome assembly from RNA-Seq  
750 data without a reference genome. *Nature biotechnology* 29, 644–652.

751 Guzinski, J., Mauger, S., Cock, J.M., Valero, M., 2016. Characterization of newly developed  
752 expressed sequence tag-derived microsatellite markers revealed low genetic diversity within and  
753 low connectivity between European *Saccharina latissima* populations. *Journal of Applied*  
754 *Phycology* 28, 3057–3070. <https://doi.org/10.1007/s10811-016-0806-7>

755 Haas, B., Papanicolaou, A., 2015. TransDecoder 5.5. 0.

756 Heinrich, S., Frickenhaus, S., Glöckner, G., Valentin, K., 2012. A comprehensive cDNA library  
757 of light- and temperature-stressed *Saccharina latissima* (Phaeophyceae). *European Journal of*  
758 *Phycology* 47, 83–94. <https://doi.org/10.1080/09670262.2012.660639>

759 Heinrich, S., Valentin, K., Frickenhaus, S., Wiencke, C., 2015. Temperature and light interactively  
760 modulate gene expression in *Saccharina latissima* (Phaeophyceae). *Journal of Phycology* 51, 93–  
761 108. <https://doi.org/10.1111/jpy.12255>

762 Hop, H., Wiencke, C., Vögele, B., Kovaltchouk, N.A., 2012. Species composition, zonation, and  
763 biomass of marine benthic macroalgae in Kongsfjorden, Svalbard. *Botanica Marina* 55, 399–414.  
764 <https://doi.org/10.1515/bot-2012-0097>

765 Hu, S., Zhang, L., Qian, S., 2020. Marine heatwaves in the Arctic region: variation in different ice  
766 covers. *Geophysical Research Letters* 47. <https://doi.org/10.1029/2020GL089329>

767 Huerta-Cepas, J., Forslund, K., Coelho, L.P., Szklarczyk, D., Jensen, L.J., Von Mering, C., Bork,  
768 P., 2017. Fast genome-wide functional annotation through orthology assignment by eggNOG-  
769 Mapper. *Molecular Biology and Evolution* 34, 2115–2122.  
770 <https://doi.org/10.1093/molbev/msx148>

771 Huerta-Cepas, J., Szklarczyk, D., Heller, D., Hernández-Plaza, A., Forslund, S.K., Cook, H.,  
772 Mende, D.R., Letunic, I., Rattei, T., Jensen, L.J., von Mering, C., Bork, P., 2019. eggNOG 5.0: a  
773 hierarchical, functionally and phylogenetically annotated orthology resource based on 5090  
774 organisms and 2502 viruses. *Nucleic Acids Research* 47, D309–D314.  
775 <https://doi.org/10.1093/nar/gky1085>

776 Iñiguez, C., Carmona, R., Lorenzo, M.R., Niell, F.X., Wiencke, C., Gordillo, F.J.L., 2016.  
777 Increased temperature, rather than elevated CO<sub>2</sub>, modulates the carbon assimilation of the Arctic  
778 kelps *Saccharina latissima* and *Laminaria solidungula*. *Marine Biology* 163, 248.  
779 <https://doi.org/10.1007/s00227-016-3024-6>

780 Karsten, U., 2012. Seaweed Acclimation to Salinity and Desiccation Stress, in: Wiencke, C.,  
781 Bischof, K. (Eds.), *Seaweed biology: novel insights into ecophysiology, ecology and utilization,*

782 ecological studies. Springer, Berlin, Heidelberg, pp. 87–107. [https://doi.org/10.1007/978-3-642-](https://doi.org/10.1007/978-3-642-28451-9_5)  
783 28451-9\_5

784 Karsten, U., 2007. Research note: salinity tolerance of Arctic kelps from Spitsbergen. *Phycological*  
785 *Research* 55, 257–262. <https://doi.org/10.1111/j.1440-1835.2007.00468.x>

786 Korb, R.E., Gerard, V.A., 2000. Nitrogen assimilation characteristics of polar seaweeds from  
787 differing nutrient environments. *Marine Ecology Progress Series* 198, 83–92.

788 Krause-Jensen, D., Archambault, P., Assis, J., Bartsch, I., Bischof, K., Filbee-Dexter, K., Dunton,  
789 K.H., Maximova, O., Ragnarsdóttir, S.B., Sejr, M.K., Simakova, U., Spiridonov, V., Wegeberg,  
790 S., Winding, M.H.S., Duarte, C.M., 2020. Imprint of climate change on pan-Arctic marine  
791 vegetation. *Frontiers in Marine Science* 7, 617324. <https://doi.org/10.3389/fmars.2020.617324>

792 Krause-Jensen, D., Duarte, C.M., 2016. Substantial role of macroalgae in marine carbon  
793 sequestration. *Nature Geoscience* 9, 737–742. <https://doi.org/10.1038/ngeo2790>

794 Krause-Jensen, D., Marbà, N., Olesen, B., Sejr, M.K., Christensen, P.B., Rodrigues, J., Renaud,  
795 P.E., Balsby, T.J.S., Rysgaard, S., 2012. Seasonal sea ice cover as principal driver of spatial and  
796 temporal variation in depth extension and annual production of kelp in Greenland. *Global Change*  
797 *Biology* 18, 2981–2994. <https://doi.org/10.1111/j.1365-2486.2012.02765.x>

798 Kwiatkowski, L., Torres, O., Bopp, L., Aumont, O., Chamberlain, M., Christian, J.R., Dunne, J.P.,  
799 Gehlen, M., Ilyina, T., John, J.G., Lenton, A., Li, H., Lovenduski, N.S., Orr, J.C., Palmieri, J.,  
800 Santana-Falcón, Y., Schwinger, J., Séférian, R., Stock, C.A., Tagliabue, A., Takano, Y., Tjiputra,  
801 J., Toyama, K., Tsujino, H., Watanabe, M., Yamamoto, A., Yool, A., Ziehn, T., 2020. Twenty-  
802 first century ocean warming, acidification, deoxygenation, and upper-ocean nutrient and primary  
803 production decline from CMIP6 model projections. *Biogeosciences* 17, 3439–3470.  
804 <https://doi.org/10.5194/bg-17-3439-2020>

805 Lebrun, A., Comeau, S., Gazeau, F., Gattuso, J.-P., 2022. Impact of climate change on Arctic  
806 macroalgal communities. *Global and Planetary Change* 103980.

807 Letunic, I., Khedkar, S., Bork, P., 2021. SMART: recent updates, new developments and status in  
808 2020. *Nucleic Acids Research* 49, D458–D460. <https://doi.org/10.1093/nar/gkaa937>

809 Li, H., Monteiro, C., Heinrich, S., Bartsch, I., Valentin, K., Harms, L., Glöckner, G., Corre, E.,  
810 Bischof, K., 2020. Responses of the kelp *Saccharina latissima* (Phaeophyceae) to the warming  
811 Arctic: from physiology to transcriptomics. *Physiologia Plantarum* 168, 5–26.  
812 <https://doi.org/10.1111/ppl.13009>

813 Li, W., Godzik, A., 2006. Cd-hit: a fast program for clustering and comparing large sets of protein  
814 or nucleotide sequences. *Bioinformatics* 22, 1658–1659.  
815 <https://doi.org/10.1093/bioinformatics/btl158>

816 Liesner, D., Fouqueau, L., Valero, M., Roleda, M.Y., Pearson, G.A., Bischof, K., Valentin, K.,  
817 Bartsch, I., 2020. Heat stress responses and population genetics of the kelp *Laminaria digitata*

818 (Phaeophyceae) across latitudes reveal differentiation among North Atlantic populations. *Ecology*  
819 and *Evolution* 10, 9144–9177. <https://doi.org/10.1002/ece3.6569>

820 [Loreau, M., Naeem, S., Inchausti, P., Bengtsson, J., Grime, J.P., Hector, A., Hooper, D.U., Huston,](#)  
821 [M.A., Raffaelli, D., Schmid, B., Tilman, D., Wardle, D.A., 2001. Biodiversity and Ecosystem](#)  
822 [Functioning: Current Knowledge and Future Challenges, \*Science\*, 294, 804–808,](#)  
823 <https://doi.org/10.1126/science.1064088>.

824 Lorenzen, C.J., 1967. Determination of chlorophyll and pheopigments: spectrophotometric  
825 equations. *Limnology and Oceanography* 12, 343–346. <https://doi.org/10.4319/lo.1967.12.2.0343>

826 Love, M.I., Huber, W., Anders, S., 2014. Moderated estimation of fold change and dispersion for  
827 RNA-seq data with DESeq2. *Genome Biology* 15, 550. [https://doi.org/10.1186/s13059-014-0550-](https://doi.org/10.1186/s13059-014-0550-8)  
828 8

829 McWilliam, J.R., Naylor, A.W., 1967. Temperature and plant adaptation. I. Interaction of  
830 temperature and light in the synthesis of chlorophyll in corn. *Plant Physiology* 42, 1711–1715.  
831 <https://doi.org/10.1104/pp.42.12.1711>

832 Meyer, C., Lea, U.S., Provan, F., Kaiser, W.M., Lillo, C., 2005. Is nitrate reductase a major player  
833 in the plant NO (nitric oxide) game? *Photosynthesis Research* 83, 181–189.  
834 <https://doi.org/10.1007/s11120-004-3548-3>

835 Millard, S.P., 2013. *EnvStats: An R Package for Environmental Statistics*. Springer, New York.  
836 ISBN 978-1-4614-8455-4, <https://www.springer.com>.

837 Miller, C.A., Urrutti, P., Gattuso, J.-P., Comeau, S., Lebrun, A., Alliouane, S., Schlegel, R.W.,  
838 [Gazeau, F., 2024a. Technical note: An autonomous flow-through salinity and temperature](#)  
839 [perturbation mesocosm system for multi-stressor experiments. \*Biogeosciences\*, 21\(1\), 315–333.](#)  
840 <https://doi.org/10.5194/bg-21-315-2024>.

841 [Miller, C. A., Gazeau, F., Lebrun, A., Gattuso, J.-P., Alliouane, S., Urrutti, P., Schlegel, R. W.,](#)  
842 [and Comeau, S., 2024. Productivity of mixed kelp communities in an Arctic fjord exhibit tolerance](#)  
843 [to a future climate. \*Science of The Total Environment\*, 930, 172571.](#)  
844 <https://doi.org/10.1016/j.scitotenv.2024.172571>

845 Mistry, J., Chuguransky, S., Williams, L., Qureshi, M., Salazar, G.A., Sonhammer, E.L.L.,  
846 Tosatto, S.C.E., Paladin, L., Raj, S., Richardson, L.J., Finn, R.D., Bateman, A., 2021. Pfam: The  
847 protein families database in 2021. *Nucleic Acids Research* 49, D412–D419.  
848 <https://doi.org/10.1093/nar/gkaa913>

849 Monteiro, C.M.M., Li, H., Bischof, K., Bartsch, I., Valentin, K.U., Corre, E., Collén, J., Harms,  
850 L., Glöckner, G., Heinrich, S., 2019. Is geographical variation driving the transcriptomic responses  
851 to multiple stressors in the kelp *Saccharina latissima*? *BMC Plant Biol* 19, 513.  
852 <https://doi.org/10.1186/s12870-019-2124-0>

Deleted:

Formatted: Font: (Default) Times New Roman, 12 pt

Formatted: Font: (Default) Times New Roman, 12 pt

Formatted: Font: (Default) Times New Roman, 12 pt

Formatted: Font: (Default) Times New Roman, 12 pt

Formatted: Font: (Default) Times New Roman, 12 pt

Formatted: Font: (Default) Times New Roman, 12 pt

Deleted: n.d. Technical note: an autonomous flow through salinity and temperature perturbation mesocosm system for multi-stressor experiments (preprint). *Biodiversity and Ecosystem Function: Marine*. <https://doi.org/10.5194/egusphere-2023-768>

Formatted: Hyperlink, Font: (Default) Times New Roman, 12 pt

Field Code Changed

Formatted: Font: (Default) Times New Roman

Formatted: Font: (Default) Times New Roman

859 Müller, R., Laepple, T., Bartsch, I., Wiencke, C., 2009. Impact of oceanic warming on the  
860 distribution of seaweeds in polar and cold-temperate waters. *Botanica Marina* 52, 617–638.  
861 <https://doi.org/10.1515/BOT.2009.080>

862 Müller, R., Wiencke, C., Bischof, K., 2008. Interactive effects of UV radiation and temperature  
863 on microstages of Laminariales (Phaeophyceae) from the Arctic and North Sea. *Climate Research*  
864 37, 203–213. <https://doi.org/10.3354/cr00762>

865 Muth, A.F., Bonsell, C., Dunton, K.H., 2021. Inherent tolerance of extreme seasonal variability in  
866 light and salinity in an Arctic endemic kelp (*Laminaria solidungula*). *Journal of Phycology* 57,  
867 1554–1562. <https://doi.org/10.1111/jpy.13187>

868 [Niedzwiedz, S., Bischof, K., 2023. Glacial retreat and rising temperatures are limiting the  
869 expansion of temperate kelp species in the future Arctic. \*Limnology and Oceanography\* 68, 816-  
870 830. <https://doi.org/10.1002/lno.12312>](https://doi.org/10.1002/lno.12312)

871 Olischläger, M., Iñiguez, C., Koch, K., Wiencke, C., Gordillo, F.J.L., 2017. Increased pCO<sub>2</sub> and  
872 temperature reveal ecotypic differences in growth and photosynthetic performance of temperate  
873 and Arctic populations of *Saccharina latissima*. *Planta* 245, 119–136.  
874 <https://doi.org/10.1007/s00425-016-2594-3>

875 Parke, M., 1948. Studies on British Laminariaceae. I. Growth in *Laminaria Saccharina* (L.)  
876 Lamour. *Journal of the Marine Biological Association of the United Kingdom* 27, 651–709.  
877 <https://doi.org/10.1017/S0025315400056071>

878 Peterson, B.J., Holmes, R.M., McClelland, J.W., Vörösmarty, C.J., Lammers, R.B., Shiklomanov,  
879 A.I., Shiklomanov, I.A., Rahmstorf, S., 2002. Increasing River Discharge to the Arctic Ocean.  
880 *Science* 298, 2171–2173. <https://doi.org/10.1126/science.1077445>

881 R Core Team, 2023. R: A language and environment for statistical computing. R Foundation for  
882 Statistical Computing, Vienna, Austria. URL <https://www.R-project.org/>

883 Renaud, P.E., Wallhead, P., Kotta, J., Włodarska-Kowalczyk, M., Bellerby, R.G., Rätsep, M.,  
884 Slagstad, D., Kukliński, P., 2019. Arctic sensitivity? Suitable habitat for benthic taxa is  
885 surprisingly robust to climate change. *Frontiers in Marine Science* 6, 538.

886 Richter-Menge, J., Overland, J.E., Mathis, J.T., Osborne, E., 2017. Arctic Report Card: Arctic  
887 shows no sign of returning to reliably frozen region of recent past decades.

888 Roleda, M., Wiencke, C., Hanelt, D., 2005. Response of Arctic kelp zoospores to ultraviolet and  
889 photosynthetically active radiation in relation to growth depth. 8th International Phycological  
890 Congress, 13-19 August 2005, Durban, South Africa.

891 Santos-Garcia, M., Ganeshram, R.S., Tuerena, R.E., Debyser, M.C.F., Husum, K., Assmy, P.,  
892 Hop, H., 2022. Nitrate isotope investigations reveal future impacts of climate change on nitrogen  
893 inputs and cycling in Arctic fjords: Kongsfjorden and Rijpfjorden (Svalbard). *Biogeosciences* 19,  
894 5973–6002. <https://doi.org/10.5194/bg-19-5973-2022>

Deleted: <https://doi.org/10.1111/jpy.13187>



896 Scherrer, K.J.N., Kortsch, S., Varpe, Ø., Weyhenmeyer, G.A., Gulliksen, B., Primicerio, R., 2019.  
897 Mechanistic model identifies increasing light availability due to sea ice reductions as cause for  
898 increasing macroalgae cover in the Arctic: light causes arctic macroalgal increase. *Limnology and*  
899 *Oceanography* 64, 330–341. <https://doi.org/10.1002/lno.11043>

900 Shiklomanov, I.A., Shiklomanov, A.I., 2003. Climatic change and the dynamics of river runoff  
901 into the Arctic Ocean. *Water Resources* 30, 593–601.

902 Simão, F.A., Waterhouse, R.M., Ioannidis, P., Kriventseva, E.V., Zdobnov, E.M., 2015. BUSCO:  
903 assessing genome assembly and annotation completeness with single-copy orthologs.  
904 *Bioinformatics* 31, 3210–3212. <https://doi.org/10.1093/bioinformatics/btv351>

905 Sivertsen, K., 1997. Geographic and environmental factors affecting the distribution of kelp beds  
906 and barren grounds and changes in biota associated with kelp reduction at sites along the  
907 Norwegian coast. *Canadian Journal of Fisheries and Aquatic Sciences* 54, 2872–2887.  
908 <https://doi.org/10.1139/f97-186>

909 Sørensen, J.G., Kristensen, T.N., Loeschcke, V., 2003. The evolutionary and ecological role of  
910 heat shock proteins: Heat shock proteins. *Ecology Letters* 6, 1025–1037.  
911 <https://doi.org/10.1046/j.1461-0248.2003.00528.x>

912 Springer, K., Lütz, C., Lütz-Meindl, U., Wendt, A., Bischof, K., 2017. Hyposaline conditions  
913 affect UV susceptibility in the Arctic kelp *Alaria esculenta* (Phaeophyceae). *Phycologia* 56, 675–  
914 685. <https://doi.org/10.2216/16-122.1>

915 Spurkland, T., Iken, K., 2011. Salinity and irradiance effects on growth and maximum  
916 photosynthetic quantum yield in subarctic *Saccharina latissima* (Laminariales, Laminariaceae).  
917 *Botanica Marina* 54. <https://doi.org/10.1515/bot.2011.042>

918 Stroeve, J.C., Markus, T., Boisvert, L., Miller, J., Barrett, A., 2014. Changes in Arctic melt season  
919 and implications for sea ice loss. *Geophysical Research Letters* 41, 1216–1225.  
920 <https://doi.org/10.1002/2013GL058951>

921 Supek, F., Bošnjak, M., Škunca, N., Šmuc, T., 2011. REVIGO Summarizes and Visualizes Long  
922 Lists of Gene Ontology Terms. *PLoS ONE* 6, e21800.  
923 <https://doi.org/10.1371/journal.pone.0021800>

924 Vihtakari M (2023). ggOceanMaps: plot data on oceanographic maps using 'ggplot2'. R package  
925 version 2.0.4, <https://mikkovihtakari.github.io/ggOceanMaps/>

926 Wiencke, C., Bartsch, I., Bischoff, B., Peters, A.F., Breeman, A.M., 1994. Temperature  
927 requirements and biogeography of Antarctic, Arctic and Amphiequatorial Seaweeds. *Botanica*  
928 *Marina* 37. <https://doi.org/10.1515/botm.1994.37.3.247>

929 Zacher, K., Bernard, M., Bartsch, I., Wiencke, C., 2016. Survival of early life history stages of  
930 Arctic kelps (Kongsfjorden, Svalbard) under multifactorial global change scenarios. *Polar Biology*  
931 39, 2009–2020. <https://doi.org/10.1007/s00300-016-1906-1>

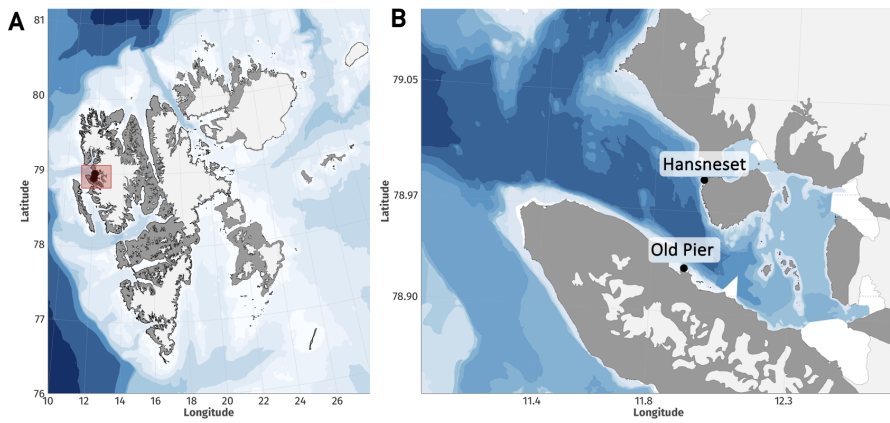
932 Zacher, K., Bernard, M., Daniel Moreno, A., Bartsch, I., 2019. Temperature mediates the outcome  
933 of species interactions in early life-history stages of two sympatric kelp species. *Marine Biology*  
934 166, 161. <https://doi.org/10.1007/s00227-019-3600-7>

935 Zhang, D.-W., Yuan, S., Xu, F., Zhu, F., Yuan, M., Ye, H.-X., Guo, H.-Q., Lv, X., Yin, Y., Lin,  
936 H.-H., 2016. Light intensity affects chlorophyll synthesis during greening process by metabolite  
937 signal from mitochondrial alternative oxidase in *A. rabidopsis*: Signalling by AOX regulates  
938 greening process. *Plant, Cell & Environment* 39, 12–25. <https://doi.org/10.1111/pce.12438>

939 **Table 1:** Temperature, salinity, and photosynthetically active radiation (PAR) during the  
 940 experiment. The T1 and T2 treatments represent future coastline exposed to runoff conditions,  
 941 whereas the T3 treatment represents future conditions on shores not exposed to runoff. The  
 942 quartiles and medians were calculated based on data acquired from 2021-07-10 for PAR and 2021-  
 943 07-16 for temperature and salinity (once the targeted treatments were reached) until the end of the  
 944 experiment.

Formatted: Font: (Default) Times New Roman, 12 pt, Bold  
 Formatted: Font: (Default) Times New Roman, 12 pt  
 Formatted: Font: (Default) Times New Roman, 12 pt  
 Formatted: Font: (Default) Times New Roman, 12 pt  
 Formatted: Font: (Default) Times New Roman, 12 pt  
 Formatted: Font: (Default) Times New Roman, 12 pt  
 Formatted: Font: (Default) Times New Roman, 12 pt  
 Deleted: Photosynthetically Active Radiation (  
 Deleted: )  
 Formatted: Font: (Default) Times New Roman, 12 pt  
 Formatted: Font: (Default) Times New Roman, 12 pt  
 Deleted: daily

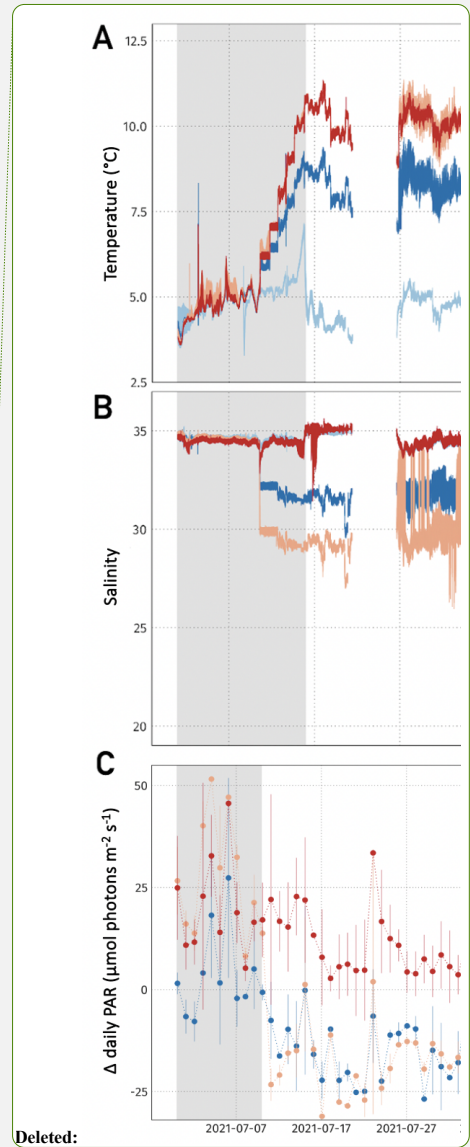
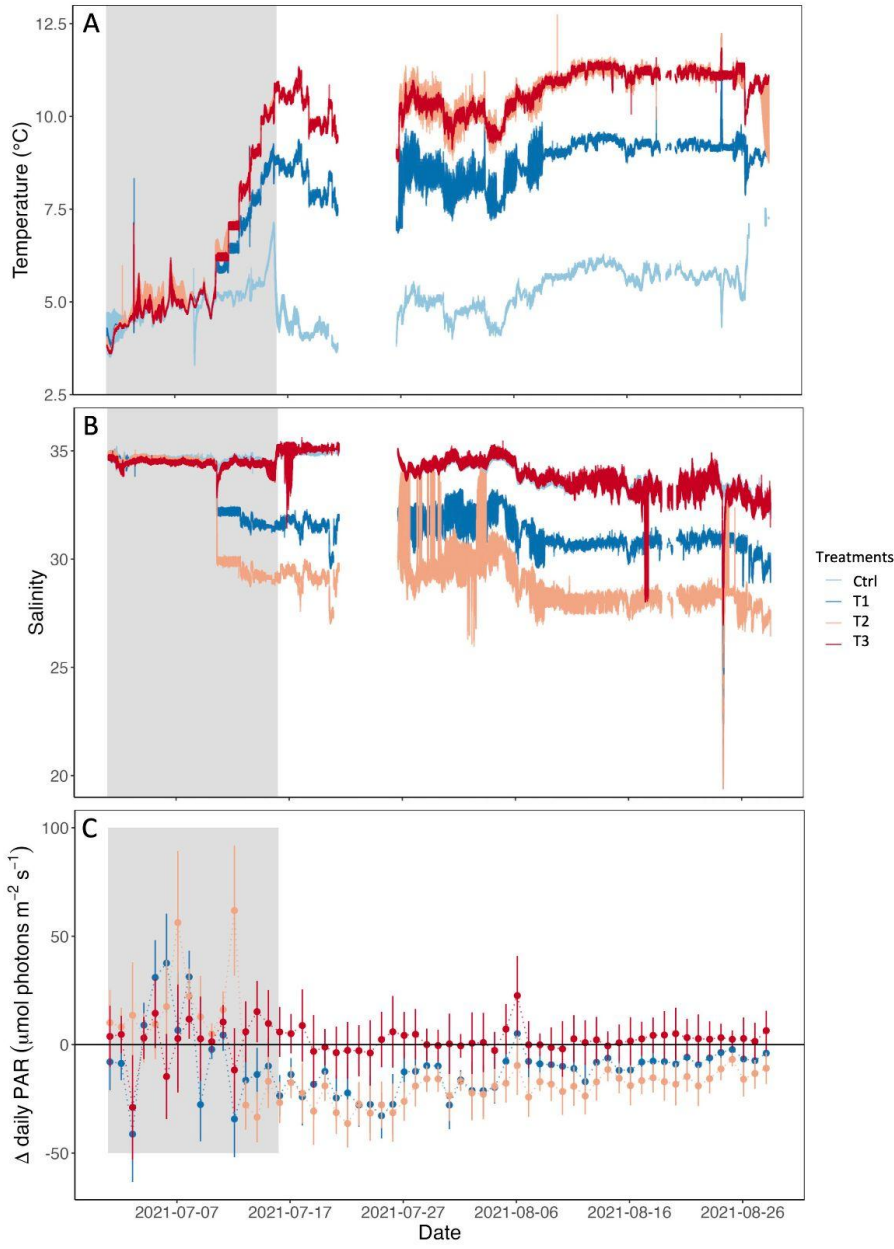
Treatment	Scenario	Temperature (°C)				Salinity				PAR ( $\mu\text{mol photons m}^{-2} \text{s}^{-1}$ )			
		$\Delta$	1st quartile	Median	3rd quartile	$\Delta$	1st quartile	Median	3rd quartile	$\Delta$	1st quartile	Median	3rd quartile
Ctrl	control	<i>in situ</i>	4.8	5.3	5.8	<i>in situ</i>	33.4	33.8	34.3	<i>in situ</i>	35.1	47.8	59.5
T1	SSP2-4.5 - coastline	+ 3.3°C	8.4	8.9	9.2	- 2.5	30.8	31.0	31.8	- 20 %	27.8	36.1	43.9
T2	SSP5-8.5 - coastline	+ 5.3°C	10.3	10.8	11.2	- 5	28.2	28.5	29.5	- 30 %	23.8	31.4	40.7
T3	SSP5-8.5 - offshore	+ 5.3°C	10.3	10.8	11.2	<i>in situ</i>	33.4	33.9	34.5	<i>in situ</i>	40.3	54.8	69.9



950

951 **Figure 1:** The study was carried out in Svalbard (A) on kelp sampled in Kongsfjorden (B) in  
 952 Hansneset and the Old Pier. Maps were created using the R package “ggOceanMaps” (Vihtakarinen,  
 953 2023).

- Formatted: Font: (Default) Times New Roman, 12 pt, Bold
- Formatted: Font: (Default) Times New Roman, 12 pt
- Formatted: Font: (Default) Times New Roman, 12 pt, Bold
- Formatted: Font: (Default) Times New Roman, 12 pt
- Formatted: Font: (Default) Times New Roman, 12 pt, Bold
- Formatted: Font: (Default) Times New Roman, 12 pt
- Formatted: Font: (Default) Times New Roman, 12 pt
- Formatted: Font: (Default) Times New Roman, 12 pt
- Formatted: Font: (Default) Times New Roman, 12 pt



956 **Figure 2: A)** Temperature, **B)** salinity, and **C)**  $\Delta$  Daily Photosynthetically Active Radiation (PAR)  
957 between the control and the treatments. Temperature and salinity were measured every minute.  
958 PAR values were integrated over 10-minute intervals and averaged over the day. The gray-shaded  
959 region corresponds to the beginning of the experiment, before the treatment conditions of  
960 temperature, salinity and irradiance were reached. A few days of temperature and salinity data  
961 were lost (from 2021-07-21 to 2021-07-26).

Formatted: Font: (Default) Times New Roman, 12 pt, Bold

Formatted: Font: (Default) Times New Roman, 12 pt

Formatted: Font: (Default) Times New Roman, 12 pt, Bold

Formatted: Font: (Default) Times New Roman, 12 pt

Formatted: Font: (Default) Times New Roman, 12 pt, Bold

Formatted: Font: (Default) Times New Roman, 12 pt

Formatted: Font: (Default) Times New Roman, 12 pt, Bold

Formatted: Font: (Default) Times New Roman, 12 pt

Deleted: ,

Deleted: ,

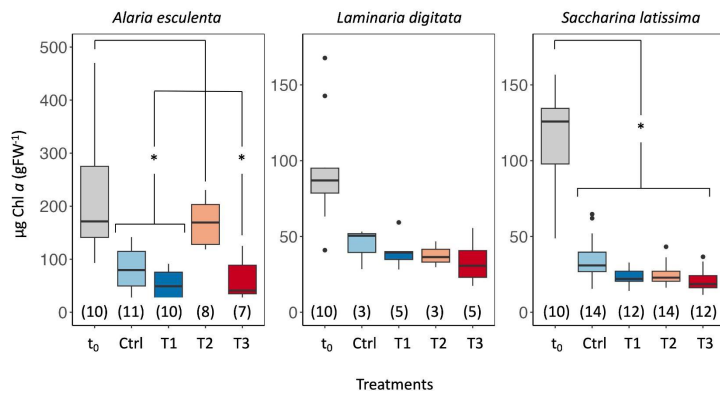
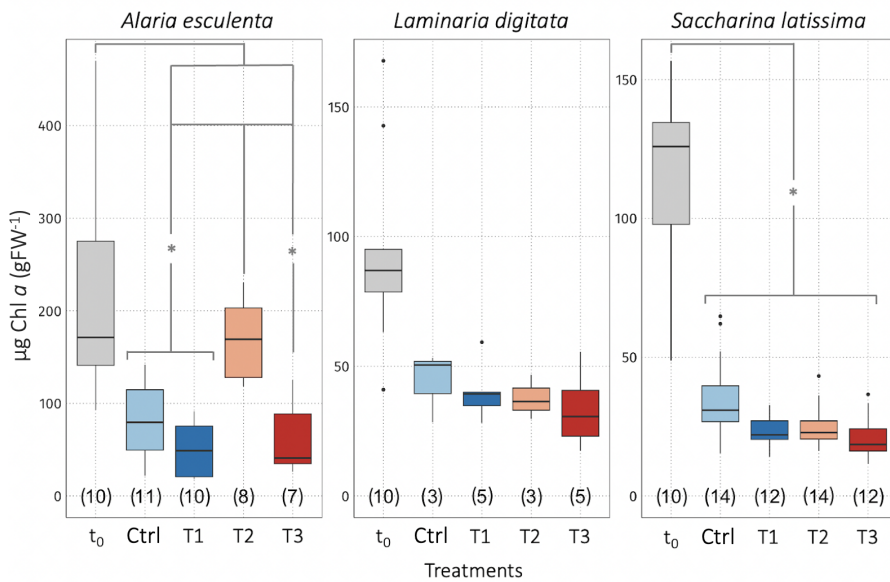
Deleted: and PAR

Formatted: Font: (Default) Times New Roman, 12 pt

Formatted: Font: (Default) Times New Roman, 12 pt

Formatted: Font: (Default) Times New Roman, 12 pt

Formatted: Font: (Default) Times New Roman, 12 pt



965

966 **Figure 3:** Chlorophyll *a* (chl *a*) content of *Alaria esculenta*, *Laminaria digitata*, and *Saccharina*  
 967 *latissima* exposed to the four treatments, expressed per unit of fresh weight (gFW). t<sub>0</sub> values  
 968 correspond to the chl *a* content at the start of the experiment, while Ctrl, T1, T2, and T3 correspond  
 969 to the final chl *a* content of organisms maintained in the respective treatments for six weeks. The  
 970 horizontal lines in each boxplot represent the median. The whiskers extend to the furthest data  
 971 points within 1.5 times the interquartile range (the top and bottom of the box). Statistically

Formatted: Font: (Default) Times New Roman, 12 pt, Bold  
 Formatted: Font: (Default) Times New Roman, 12 pt

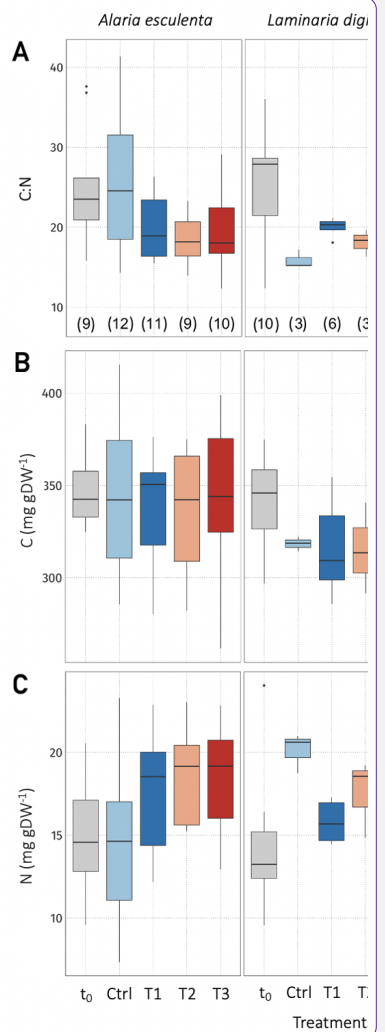
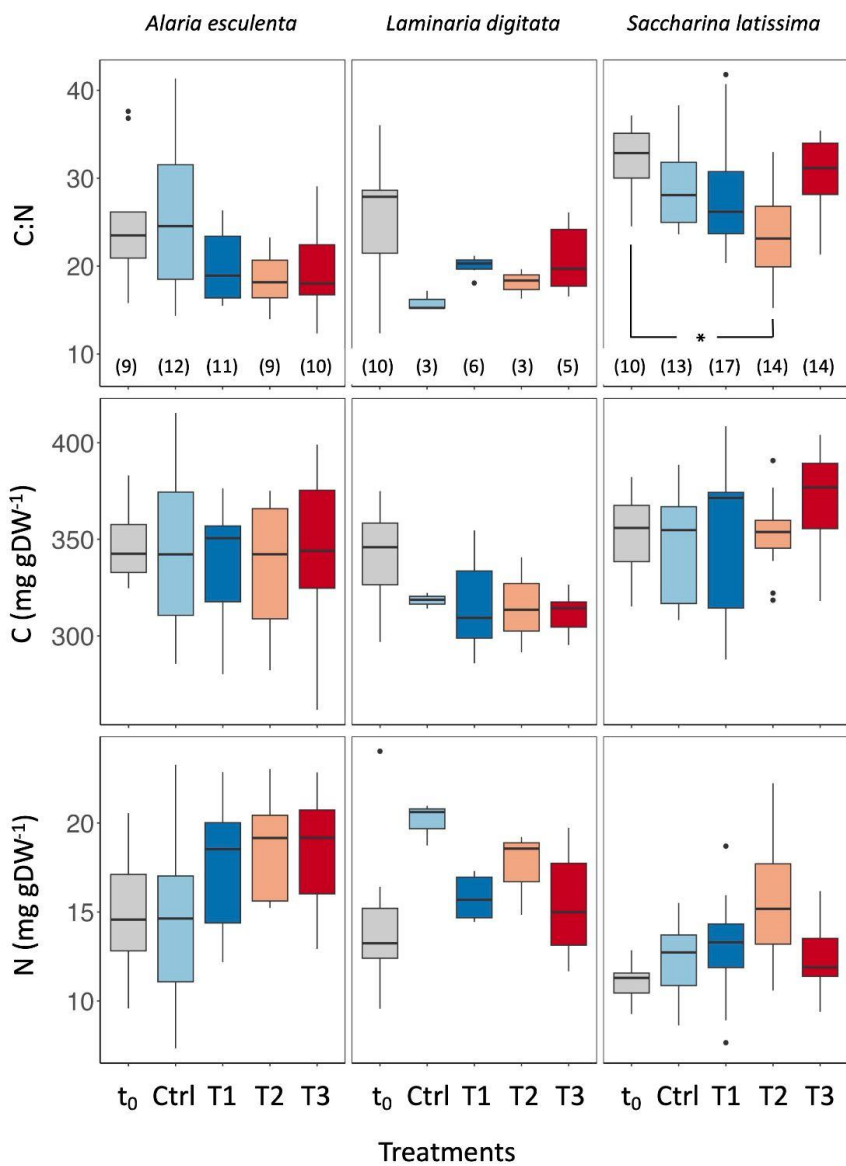


972 significant differences are shown with an asterisk ( $p < 0.05$ ). The number in parentheses below  
973 each boxplot corresponds to the sample size.

Formatted: Font: (Default) Times New Roman, 12 pt, Italic

Formatted: Font: (Default) Times New Roman, 12 pt

Deleted:



Deleted:

Deleted: 11

979 **Figure 4: A)** Carbon:nitrogen (C:N), **B)** carbon contents, and **C)** nitrogen contents of *Alaria*  
980 *esculenta*, *Laminaria digitata*, and *Saccharina latissima* exposed to the four treatments, expressed  
981 per unit of dry weight (gDW).  $t_0$  values correspond to samples taken at the start of the experiment,  
982 while Ctrl, T1, T2, and T3 correspond to the final values from organisms maintained in the  
983 respective treatments for six weeks. The horizontal lines in each boxplot represent the median. The  
984 whiskers extend to the furthest data points within 1.5 times the interquartile range (the top and  
985 bottom of the box). Statistically significant differences are shown with an asterisk ( $p < 0.05$ ). The  
986 number in parentheses below each boxplot in **(A)** corresponds to the sample size, respectively the  
987 same in **(B)** and **(C)**.

Formatted: Font: (Default) Times New Roman, 12 pt, Bold

Formatted: Font: (Default) Times New Roman, 12 pt

Formatted: Font: (Default) Times New Roman, 12 pt, Bold

Formatted: Font: (Default) Times New Roman, 12 pt

Formatted: Font: (Default) Times New Roman, 12 pt, Bold

Formatted: Font: (Default) Times New Roman, 12 pt

Formatted: Font: (Default) Times New Roman, 12 pt, Bold

Formatted: Font: (Default) Times New Roman, 12 pt

Formatted: Font: (Default) Times New Roman, 12 pt, Italic

Formatted: Font: (Default) Times New Roman, 12 pt

Formatted: Font: (Default) Times New Roman, 12 pt, Bold

Formatted: Font: (Default) Times New Roman, 12 pt

Formatted: Font: (Default) Times New Roman, 12 pt, Bold

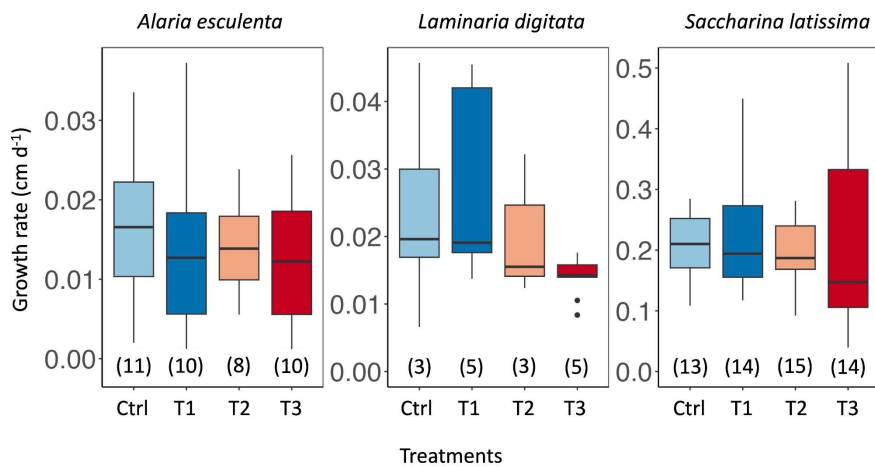
Formatted: Font: (Default) Times New Roman, 12 pt

Formatted: Font: (Default) Times New Roman, 12 pt, Bold

Formatted: Font: (Default) Times New Roman, 12 pt

Formatted: Font: (Default) Times New Roman, 12 pt, Bold

Formatted: Font: (Default) Times New Roman, 12 pt



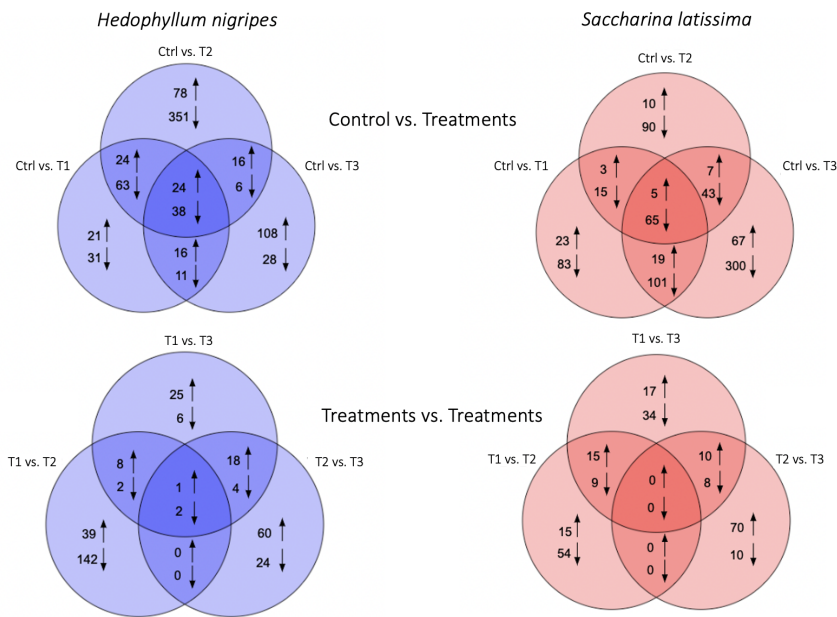
988

989 **Figure 5:** Growth rate of *Alaria esculenta*, *Laminaria digitata*, and *Saccharina latissima* exposed  
 990 to the four treatments during six weeks. The horizontal lines in each boxplot represent the median.  
 991 The horizontal lines in each boxplot represent the median. The whiskers extend to the furthest data  
 992 points within 1.5 times the interquartile range (the top and bottom of the box). The number in  
 993 parentheses below each boxplot corresponds to the sample size.

Deleted: <object>

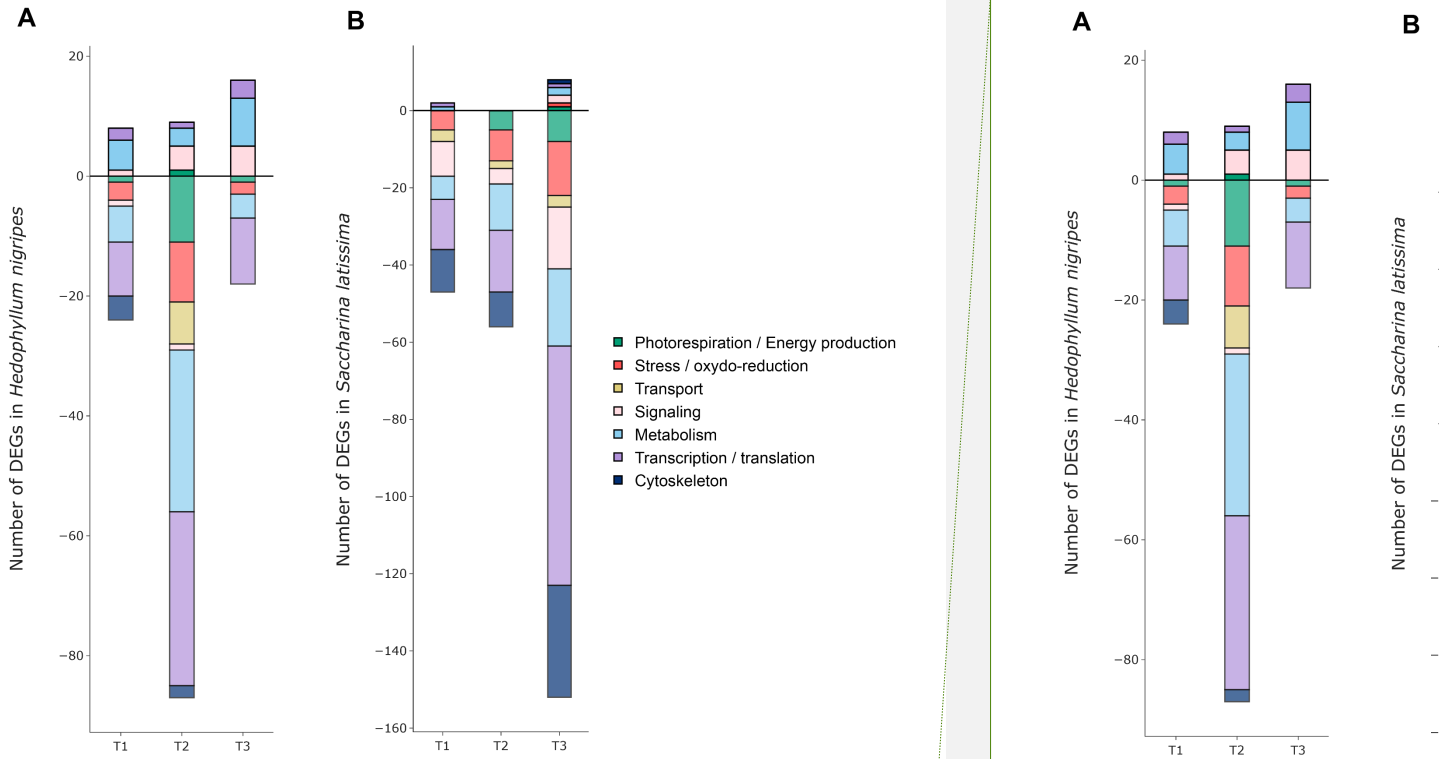
Formatted: Font: (Default) Times New Roman, 12 pt, Bold

Formatted: Font: (Default) Times New Roman, 12 pt



995 **Figure 6:** Venn diagrams of differentially up-regulated (↑) and down-regulated (↓) genes of  
 996 *Saccharina latissima* and *Hedophyllum nigripes* between the control and the treatments (T1, T2,  
 997 and T3) and between treatments.

Formatted: Font: (Default) Times New Roman, 12 pt, Bold  
 Formatted: Font: (Default) Times New Roman, 12 pt  
 Formatted: Font: (Default) Times New Roman, 12 pt  
 Formatted: Font: (Default) Times New Roman, 12 pt  
 Formatted: Font: (Default) Times New Roman, 12 pt



998

999 **Figure 7:** Number of classified differentially expressed genes (DEGs) in **A)** *Hedophyllum nigripes*  
 1000 and **B)** *Saccharina latissima* in response to T1, T2, and T3. The upper part of the graph displays  
 1001 up-regulated DEGs and the lower part down-regulated DEGs. Genes were classified with their  
 1002 Pfam and EggNOG annotations (see 2.7).

Deleted:

Formatted: Font: (Default) Times New Roman, 12 pt, Bold

Formatted: Font: (Default) Times New Roman, 12 pt

Formatted: Font: (Default) Times New Roman, 12 pt, Bold

Formatted: Font: (Default) Times New Roman, 12 pt

Formatted: Font: (Default) Times New Roman, 12 pt, Bold

Formatted: Font: (Default) Times New Roman, 12 pt

1004 **Table S1:** Tools and parameters used for transcriptomic data processing.  
 1005

Formatted: Font: (Default) Times New Roman, 12 pt, Bold

Formatted: Font: (Default) Times New Roman, 12 pt

Tool	Version	Arguments and parameters
FastQC	0.11.7	-o \$outputDirectory
Trimmomatic	0.39	PE -threads 10 -phred33 -trimlog LEADING:3 TRAILING:3 SLIDINGWINDOW:4:15 MINLEN:36 TruSeq3-PE.fa:2:30:10
Trinity	2.14.0	--seqType fq --max_memory 128G --samples_file \$sampleFiles --CPU 32 --output \$outputDirectory --full_cleanup
CD-HIT	4.8.1	-i \$transcriptome -o \$output -c 0.95 -n 8
rnaSPAdes	3.14.1	--pe1-1 \$seq1 --pe1-2 \$seq2 [...] --pe4-1 \$seq7 --pe4-2 \$seq8 -o \$output_directory
BUSCO	5.4.3	--in \$transcriptome --out \$output -c 24 -l /\$pathDB/eukaryota_odb10 --config \$config -- mode transcriptome
Kallisto	0.46.0	quant -i \$index -o \$outputDirectory -b 100 -t 16 \$seq1 \$seq2
DESeq2	1.34.0	Counts recovery via txImport (files=DesignFile, type='Kallisto', tx2gene=tx2geneFile) Contrasts depends on biological questions with alpha=0.05
TransDecoder	5.5.0	LongOrfs : \$transcriptome Predict : \$transcriptome
HMMER	3.3	--domtblout \$output -E 1e-10 --cpu 16 \$pfamDB \$transdecoderLongestOrf
eggNOG- mapper	2.1.10	-i \$transdecoderLongestOrf -o \$eggnogAnnot
Ontologizer	2.1	-a \$associationFile -g \$goDB -s \$studySamples -p \$populationFile -c Parent-Child- Union -o \$outputDirectory -d 0.05 -r 1000



1007 **Table S2:** Analysis of deviance (Type II Wald chi-square tests) in a linear mixed model with  
1008 a hierarchical structure to predict the chlorophyll a contents.

**Formatted:** Font: (Default) Times New Roman, 12 pt, Bold

**Formatted:** Font: (Default) Times New Roman, 12 pt

	Chisq	Df	Pr(>Chisq)
species	91.310	2	<2.2e-16 ***
treatment	98.991	4	<2.2e-16 ***
species:treatment	39.729	8	3.599e-06 ***

1009

1010 **Table S3:** Pairwise comparisons of the chlorophyll *a* values calculated by the method of  
 1011 Tukey on a linear mixed model with a hierarchical structure (fixed factors: treatment and  
 1012 species, random factor: mesocosm). The p-values in bold (< 0.05) support the hypothesis that  
 1013 there is a significant difference in the pair. AE: *Alaria esculenta*, LD: *Laminaria digitata*, SL:  
 1014 *Saccharina latissima*.  
 1015

Species	Treatment	vs.	Species	Treatment	estimate	SE	df	t.ratio	p.value
AE	to	-	LD	to	124.75	18.6	117.0	6.708	<.0001
AE	to	-	SL	to	104.37	18.6	117.0	5.612	<.0001
AE	to	-	AE	Ctrl	136.06	19.0	22.9	7.146	<.0001
AE	to	-	AE	T1	167.96	19.3	25.6	8.706	<.0001
AE	to	-	AE	T2	48.68	20.4	30.6	2.388	0.5405
AE	to	-	AE	T3	155.52	21.2	33.5	7.325	<.0001
LD	to	-	SL	to	-20.38	18.6	117.0	-1.096	0.9988
LD	to	-	LD	Ctrl	49.65	27.8	69.5	1.783	0.8967
LD	to	-	LD	T1	54.29	24.0	38.6	2.260	0.6231
LD	to	-	LD	T2	56.08	27.8	69.5	2.014	0.7829
LD	to	-	LD	T3	60.95	23.5	43.6	2.588	0.4048
SL	to	-	LD	Ctrl	70.03	27.8	69.5	2.515	0.4437
SL	to	-	SL	Ctrl	79.06	18.0	20.0	4.396	<b>0.0158</b>
SL	to	-	SL	T1	90.64	18.5	22.2	4.887	<b>0.0044</b>
SL	to	-	SL	T2	89.20	18.0	19.9	4.953	<b>0.0049</b>
SL	to	-	SL	T3	93.45	18.6	21.9	5.019	<b>0.0034</b>
AE	Ctrl	-	LD	Ctrl	38.33	27.2	117.8	1.409	0.9850
AE	Ctrl	-	SL	Ctrl	47.36	17.0	118.9	2.779	0.2727
AE	Ctrl	-	AE	T1	31.89	18.4	118.7	1.733	0.9184

Formatted: Font: (Default) Times New Roman, 12 pt, Bold

Formatted: Font: (Default) Times New Roman, 12 pt

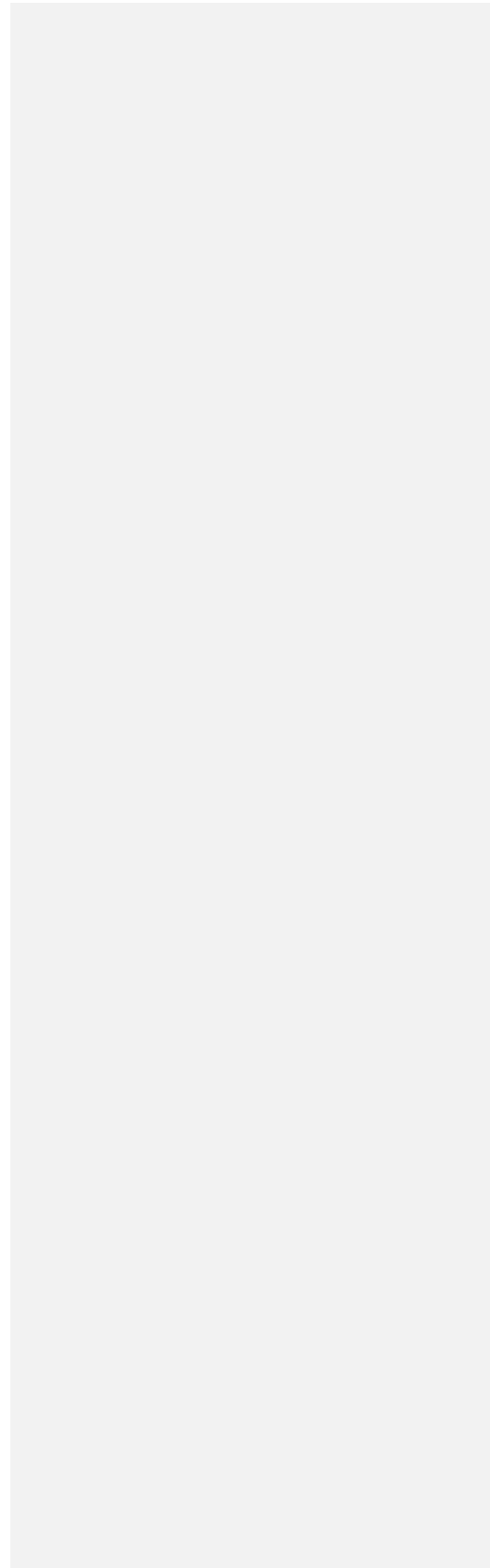
Formatted: Font: (Default) Times New Roman, 12 pt, Italic

Formatted: Font: (Default) Times New Roman, 12 pt

AE	Ctrl	-	AE	T2	-87.38	19.4	117.9	-4.497	<b>0.0015</b>
AE	Ctrl	-	AE	T3	19.46	20.3	118.6	0.958	0.9997
LD	Ctrl	-	SL	Ctrl	9.04	26.5	117.2	0.341	1.0000
LD	Ctrl	-	LD	T1	4.64	30.9	119.0	0.150	1.0000
LD	Ctrl	-	LD	T2	6.43	34.0	117.0	0.190	1.0000
LD	Ctrl	-	LD	T3	11.30	30.5	118.0	0.370	1.0000
SL	Ctrl	-	LD	T1	-4.40	22.6	115.7	-0.194	1.0000
SL	Ctrl	-	SL	T1	11.58	16.5	118.4	0.702	1.0000
SL	Ctrl	-	SL	T2	10.14	15.7	117.4	0.644	1.0000
SL	Ctrl	-	SL	T3	14.39	16.4	117.3	0.878	0.9999
AE	T1	-	LD	T1	11.08	23.6	117.3	0.469	1.0000
AE	T1	-	SL	T1	27.05	17.9	118.0	1.511	0.9722
AE	T1	-	AE	T2	-119.27	19.7	117.2	-6.040	<b>&lt;.0001</b>
AE	T1	-	AE	T3	-12.43	20.7	118.6	-0.600	1.0000
LD	T1	-	SL	T1	15.98	22.6	119.0	0.707	1.0000
LD	T1	-	LD	T2	1.79	30.9	119.0	0.058	1.0000
LD	T1	-	LD	T3	6.66	26.4	118.0	0.252	1.0000
SL	T1	-	SL	T2	-1.44	16.6	118.8	-0.087	1.0000
SL	T1	-	SL	T3	2.81	17.2	118.9	0.163	1.0000
AE	T2	-	LD	T2	132.14	28.2	117.1	4.691	<b>0.0007</b>
AE	T2	-	SL	T2	144.88	18.4	117.1	7.856	<b>&lt;.0001</b>
AE	T2	-	AE	T3	106.84	21.7	118.4	4.920	<b>0.0003</b>
LD	T2	-	SL	T2	12.74	26.5	117.3	0.481	1.0000
LD	T2	-	LD	T3	4.87	30.5	118.0	0.159	1.0000
SL	T2	-	SL	T3	4.25	16.4	117.6	0.259	1.0000

AE	T3	-	LD	T3	30.17	24.5	118.1	1.231	0.9959
AE	T3	-	SL	T3	42.29	20.2	119.0	2.091	0.7381
LD	T3	-	SL	T3	12.12	22.6	119.0	0.537	1.0000

1016



1017 **Table S4:** C:N ratios (A), carbon contents (B), and nitrogen contents as a function of the  
 1018 treatment were investigated with an analysis of deviance (Type II Wald chi-square tests) in a  
 1019 linear mixed model with a hierarchical structure.  
 1020

**A**

	Chisq	Df	Pr(>Chisq)
species	61.003	2	5.667e-14 ***
treatment	29.275	4	6.872e-06 ***
species:treatment	11.285	8	0.1861

**B**

	Chisq	Df	Pr(>Chisq)
species	23.8694	2	6.559e-06 ***
treatment	3.8547	4	0.4260
species:treatment	6.0497	8	0.6417

**C**

	Chisq	Df	Pr(>Chisq)
species	51.647	2	6.096e-12 ***
treatment	25.979	4	3.196e-05 ***
species:treatment	14.373	8	0.07254

1021

Formatted: Font: (Default) Times New Roman, 12 pt, Bold

Formatted: Font: (Default) Times New Roman, 12 pt

Formatted: Font: (Default) Times New Roman, 12 pt, Bold

Formatted: Font: (Default) Times New Roman, 12 pt

Formatted: Font: (Default) Times New Roman, 12 pt, Bold

Formatted: Font: (Default) Times New Roman, 12 pt

1022 **Table S5:** Pairwise comparisons of **A)** the C:N ratios, **B)** the carbon contents, **C)** the nitrogen  
 1023 contents calculated by the method of Tukey on a linear mixed model with a hierarchical  
 1024 structure (fixed factors: treatment and species, random factor: mesocosm). The p-values in  
 1025 bold ( $p < 0.05$ ) indicates a significant difference in the pair. AE: *Alaria esculenta*, LD:  
 1026 *Laminaria digitata*, SL: *Saccharina latissima*.  
 1027

A	Species	Treatment	vs.	Species	Treatment	estimate	SE	df	t.ratio	p.value
	AE	to	-	LD	to	-0.1152	2.63	125.0	-0.044	1.0000
	AE	to	-	SL	to	-6.7996	2.56	125.0	-2.654	0.3458
	AE	to	-	AE	Ctrl	-0.4640	2.47	41.0	-0.187	1.0000
	AE	to	-	AE	T1	5.2689	2.51	45.0	2.100	0.7276
	AE	to	-	AE	T2	6.7233	2.83	58.0	2.378	0.5403
	AE	to	-	AE	T3	5.8060	2.56	47.8	2.264	0.6201
	LD	to	-	SL	to	-6.6845	2.56	125.0	-2.609	0.3746
	LD	to	-	LD	Ctrl	9.4646	3.72	98.2	2.546	0.4190
	LD	to	-	LD	T1	5.3231	2.99	58.9	1.783	0.8955
	LD	to	-	LD	T2	7.2351	3.72	98.2	1.946	0.8236
	LD	to	-	LD	T3	4.4934	3.14	69.9	1.431	0.9814
	SL	to	-	SL	Ctrl	2.9358	2.36	36.1	1.246	0.9937
	SL	to	-	SL	T1	3.6898	2.22	31.4	1.659	0.9302
	SL	to	-	SL	T2	8.5439	2.32	34.5	3.686	<b>0.0453</b>
	SL	to	-	SL	T3	1.5997	2.36	35.2	0.677	1.0000
	AE	Ctrl	-	LD	Ctrl	9.8134	3.61	125.6	2.718	0.3066
	AE	Ctrl	-	SL	Ctrl	-3.3998	2.28	126.8	-1.490	0.9755
	AE	Ctrl	-	AE	T1	5.7328	2.34	126.1	2.449	0.4841
	AE	Ctrl	-	AE	T2	7.1873	2.67	126.2	2.694	0.3206
	AE	Ctrl	-	AE	T3	6.2700	2.41	126.7	2.599	0.3810

Formatted: Font: (Default) Times New Roman, 12 pt, Bold

Formatted: Font: (Default) Times New Roman, 12 pt

Formatted: Font: (Default) Times New Roman, 12 pt, Bold

Formatted: Font: (Default) Times New Roman, 12 pt

Formatted: Font: (Default) Times New Roman, 12 pt, Bold

Formatted: Font: (Default) Times New Roman, 12 pt

Formatted: Font: (Default) Times New Roman, 12 pt, Bold

Formatted: Font: (Default) Times New Roman, 12 pt

Formatted: Font: (Default) Times New Roman, 12 pt, Bold

Formatted: Font: (Default) Times New Roman, 12 pt

Formatted: Font: (Default) Times New Roman, 12 pt, Bold

Formatted: Font: (Default) Times New Roman, 12 pt

Formatted: Font: (Default) Times New Roman, 12 pt

LD	Ctrl	-	SL	Ctrl	-13.2133	3.58	125.5	-3.692	<b>0.0247</b>
LD	Ctrl	-	LD	T1	-4.1415	3.98	126.7	-1.041	0.9993
LD	Ctrl	-	LD	T2	-2.2295	4.55	125.0	-0.490	1.0000
LD	Ctrl	-	LD	T3	-4.9712	4.09	126.2	-1.214	0.9965
SL	Ctrl	-	SL	T1	0.7539	2.07	126.7	0.363	1.0000
SL	Ctrl	-	SL	T2	5.6081	2.17	126.8	2.581	0.3927
SL	Ctrl	-	SL	T3	-1.3361	2.21	126.6	-0.606	1.0000
AE	T1	-	LD	T1	-0.0609	2.90	126.3	-0.021	1.0000
AE	T1	-	SL	T1	-8.3787	2.16	125.5	-3.875	<b>0.0136</b>
AE	T1	-	AE	T2	1.4545	2.72	126.7	0.535	1.0000
AE	T1	-	AE	T3	0.5372	2.44	125.2	0.220	1.0000
LD	T1	-	SL	T1	-8.3178	2.69	126.9	-3.086	0.1367
LD	T1	-	LD	T2	1.9120	3.98	126.7	0.481	1.0000
LD	T1	-	LD	T3	-0.8297	3.38	125.1	-0.246	1.0000
SL	T1	-	SL	T2	4.8542	2.02	126.2	2.398	0.5214
SL	T1	-	SL	T3	-2.0900	2.08	127.0	-1.004	0.9995
AE	T2	-	LD	T2	0.3966	3.86	125.7	0.103	1.0000
AE	T2	-	SL	T2	-4.9791	2.61	126.9	-1.907	0.8453
AE	T2	-	AE	T3	-0.9173	2.78	126.8	-0.330	1.0000
LD	T2	-	SL	T2	-5.3757	3.55	125.4	-1.513	0.9721
LD	T2	-	LD	T3	-2.7417	4.09	126.2	-0.670	1.0000
SL	T2	-	SL	T3	-6.9442	2.15	125.7	-3.223	0.0967
AE	T3	-	LD	T3	-1.4278	3.09	126.9	-0.462	1.0000
AE	T3	-	SL	T3	-11.0059	2.36	126.1	-4.669	<b>0.0007</b>
LD	T3	-	SL	T3	-9.5782	3.02	125.3	-3.173	0.1101

<b>B</b>	Species	Treatment	vs.	Species	Treatment	estimate	SE	df	t.ratio	p.value
	AE	to	-	LD	to	5.634	14.1	125.0	0.400	1.0000
	AE	to	-	SL	to	-6.839	13.7	125.0	-0.498	1.0000
	AE	to	-	AE	Ctrl	3.002	13.3	41.0	0.226	1.0000
	AE	to	-	AE	T1	8.934	13.4	45.0	0.664	1.0000
	AE	to	-	AE	T2	10.408	15.2	58.0	0.687	1.0000
	AE	to	-	AE	T3	1.157	13.7	47.8	0.084	1.0000
	LD	to	-	SL	to	-12.473	13.7	125.0	-0.908	0.9999
	LD	to	-	LD	Ctrl	21.981	19.9	98.2	1.103	0.9987
	LD	to	-	SL	Ctrl	-7.587	13.0	39.6	-0.583	1.0000
	LD	to	-	LD	T1	24.351	16.0	58.9	1.521	0.9679
	LD	to	-	LD	T2	25.098	19.9	98.2	1.259	0.9947
	LD	to	-	LD	T3	28.694	16.8	69.9	1.705	0.9244
	SL	to	-	SL	Ctrl	4.886	12.6	36.1	0.387	1.0000
	SL	to	-	SL	T1	0.176	11.9	31.4	0.015	1.0000
	SL	to	-	SL	T2	-0.691	12.4	34.5	-0.056	1.0000
	SL	to	-	SL	T3	-18.336	12.7	35.2	-1.447	0.9761
	AE	Ctrl	-	LD	Ctrl	24.612	19.4	125.6	1.272	0.9944
	AE	Ctrl	-	SL	Ctrl	-4.956	12.2	126.8	-0.405	1.0000
	AE	Ctrl	-	AE	T1	5.932	12.5	126.1	0.473	1.0000
	AE	Ctrl	-	AE	T2	7.406	14.3	126.2	0.518	1.0000
	AE	Ctrl	-	LD	T2	27.730	19.4	125.6	1.433	0.9827
	AE	Ctrl	-	AE	T3	-1.845	12.9	126.7	-0.143	1.0000
	LD	Ctrl	-	SL	Ctrl	-29.568	19.2	125.5	-1.541	0.9674

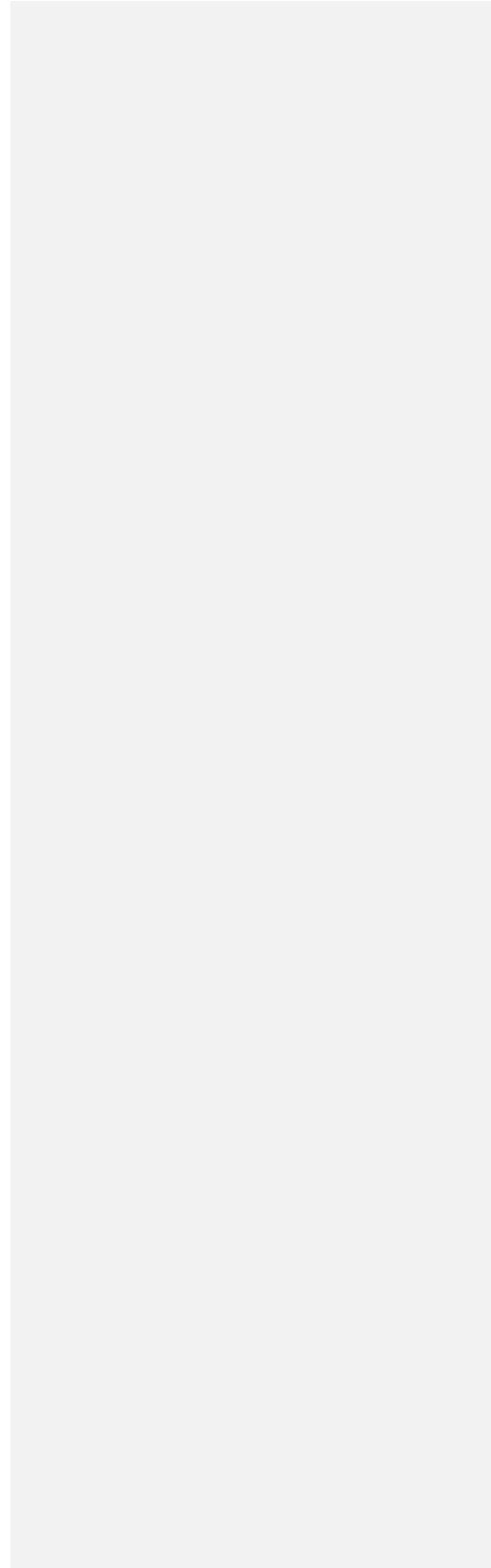


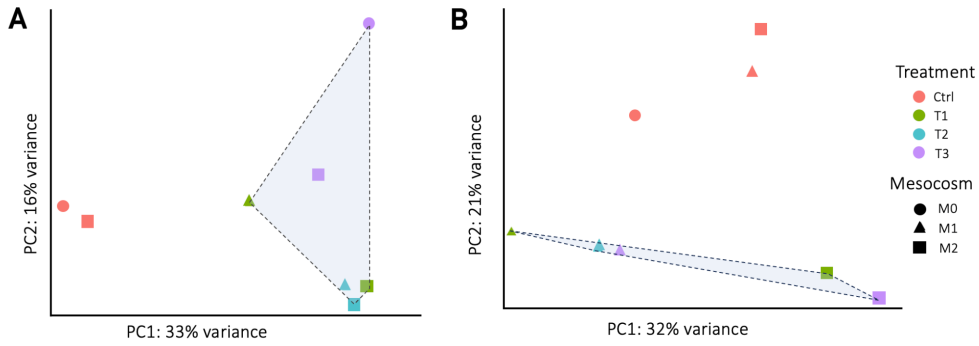
LD	Ctrl	-	LD	T1	2.370	21.3	126.7	0.111	1.0000
LD	Ctrl	-	SL	T1	-34.278	18.7	125.0	-1.831	0.8810
LD	Ctrl	-	LD	T2	3.117	24.4	125.0	0.128	1.0000
LD	Ctrl	-	LD	T3	6.713	22.0	126.2	0.306	1.0000
SL	Ctrl	-	SL	T1	-4.710	11.1	126.7	-0.424	1.0000
SL	Ctrl	-	SL	T2	-5.577	11.6	126.8	-0.479	1.0000
SL	Ctrl	-	SL	T3	-23.222	11.8	126.6	-1.963	0.8153
AE	T1	-	LD	T1	21.051	15.5	126.3	1.355	0.9896
AE	T1	-	SL	T1	-15.598	11.6	125.5	-1.345	0.9903
AE	T1	-	AE	T2	1.474	14.6	126.7	0.101	1.0000
AE	T1	-	AE	T3	-7.777	13.1	125.2	-0.595	1.0000
LD	T1	-	SL	T1	-36.648	14.4	126.9	-2.537	0.4227
LD	T1	-	LD	T2	0.747	21.3	126.7	0.035	1.0000
LD	T1	-	LD	T3	4.343	18.1	125.1	0.240	1.0000
SL	T1	-	LD	T2	37.396	18.7	125.0	1.997	0.7962
SL	T1	-	SL	T2	-0.867	10.9	126.2	-0.080	1.0000
SL	T1	-	SL	T3	-18.512	11.2	127.0	-1.658	0.9414
AE	T2	-	AE	T3	-9.251	14.9	126.8	-0.621	1.0000
LD	T2	-	SL	T2	-38.262	19.1	125.4	-2.008	0.7896
LD	T2	-	LD	T3	3.596	22.0	126.2	0.164	1.0000
SL	T2	-	SL	T3	-17.645	11.6	125.7	-1.528	0.9697
AE	T3	-	LD	T3	33.171	16.6	126.9	2.001	0.7940
AE	T3	-	SL	T3	-26.332	12.6	126.1	-2.084	0.7429
LD	T3	-	SL	T3	-59.503	16.2	125.3	-3.677	<b>0.0259</b>

C	Species	Treatment	vs.	Species	Treatment	estimate	SE	df	t.ratio	p.value
	AE	to	-	LD	to	0.2529	1.44	125.0	0.176	1.0000
	AE	to	-	SL	to	3.5217	1.40	125.0	2.508	0.4423
	AE	to	-	AE	Ctrl	0.0322	1.36	41.0	0.024	1.0000
	AE	to	-	AE	T1	-2.8539	1.37	45.0	-2.077	0.7425
	AE	to	-	AE	T2	-3.8535	1.55	58.0	-2.487	0.4650
	AE	to	-	AE	T3	-3.8036	1.41	47.8	-2.707	0.3318
	LD	to	-	SL	to	3.2689	1.40	125.0	2.328	0.5718
	LD	to	-	LD	Ctrl	-5.7111	2.04	98.2	-2.804	0.2626
	LD	to	-	LD	T1	-1.4098	1.64	58.9	-0.862	0.9999
	LD	to	-	LD	T2	-3.1407	2.04	98.2	-1.542	0.9665
	LD	to	-	LD	T3	-1.0560	1.72	69.9	-0.614	1.0000
	SL	to	-	SL	Ctrl	-1.1248	1.29	36.1	-0.871	0.9999
	SL	to	-	SL	T1	-1.8877	1.22	31.4	-1.550	0.9576
	SL	to	-	SL	T2	-4.5131	1.27	34.5	-3.554	0.0622
	SL	to	-	SL	T3	-1.3004	1.30	35.2	-1.004	0.9993
	AE	Ctrl	-	LD	Ctrl	-5.4905	1.98	125.6	-2.776	0.2740
	AE	Ctrl	-	SL	Ctrl	2.3647	1.25	126.8	1.892	0.8529
	AE	Ctrl	-	AE	T1	-2.8861	1.28	126.1	-2.251	0.6282
	AE	Ctrl	-	AE	T2	-3.8856	1.46	126.2	-2.659	0.3426
	AE	Ctrl	-	AE	T3	-3.8358	1.32	126.7	-2.902	0.2102
	LD	Ctrl	-	SL	Ctrl	7.8552	1.96	125.5	4.006	<b>0.0087</b>
	LD	Ctrl	-	LD	T1	4.3014	2.18	126.7	1.973	0.8098
	LD	Ctrl	-	LD	T2	2.5704	2.49	125.0	1.030	0.9994
	LD	Ctrl	-	LD	T3	4.6552	2.24	126.2	2.075	0.7485

SL	Ctrl	-	SL	T1	-0.7629	1.14	126.7	-0.671	1.0000
SL	Ctrl	-	SL	T2	-3.3883	1.19	126.8	-2.846	0.2368
SL	Ctrl	-	SL	T3	-0.1756	1.21	126.6	-0.145	1.0000
AE	T1	-	LD	T1	1.6970	1.59	126.3	1.069	0.9991
AE	T1	-	SL	T1	4.4880	1.18	125.5	3.788	<b>0.0181</b>
AE	T1	-	AE	T2	-0.9995	1.49	126.7	-0.670	1.0000
AE	T1	-	AE	T3	-0.9497	1.34	125.2	-0.711	1.0000
LD	T1	-	SL	T1	2.7910	1.48	126.9	1.890	0.8536
LD	T1	-	AE	T2	-2.6966	1.72	126.8	-1.568	0.9623
LD	T1	-	LD	T2	-1.7310	2.18	126.7	-0.794	1.0000
LD	T1	-	LD	T3	0.3538	1.85	125.1	0.191	1.0000
SL	T1	-	SL	T2	-2.6254	1.11	126.2	-2.367	0.5439
SL	T1	-	SL	T3	0.5873	1.14	127.0	0.515	1.0000
AE	T2	-	LD	T2	0.9656	2.12	125.7	0.456	1.0000
AE	T2	-	SL	T2	2.8621	1.43	126.9	2.001	0.7942
AE	T2	-	AE	T3	0.0498	1.52	126.8	0.033	1.0000
LD	T2	-	SL	T2	1.8965	1.95	125.4	0.974	0.9997
LD	T2	-	LD	T3	2.0848	2.24	126.2	0.929	0.9998
SL	T2	-	SL	T3	3.2127	1.18	125.7	2.721	0.3047
AE	T3	-	LD	T3	3.0005	1.69	126.9	1.771	0.9051
AE	T3	-	SL	T3	6.0250	1.29	126.1	4.665	<b>0.0007</b>
LD	T3	-	SL	T3	3.0244	1.65	125.3	1.829	0.8818

1029 **Figure S1 missing**





1030 **Fig. S2:** Principal Component Analysis of the expressed genes in the control and treatments of  
 1031 **A)** *Hedophyllum nigripes* and **B)** *Saccharina latissima*. Treatments T1, T2, and T3 are grouped  
 1032 in the blue geometrical figures.

Formatted: Font: (Default) Times New Roman, 12 pt, Bold

Formatted: Font: (Default) Times New Roman, 12 pt

Formatted: Font: (Default) Times New Roman, 12 pt, Bold

Formatted: Font: (Default) Times New Roman, 12 pt

Formatted: Font: (Default) Times New Roman, 12 pt, Bold

Formatted: Font: (Default) Times New Roman, 12 pt

Formatted: Font: (Default) Times New Roman, 12 pt

Formatted: Font: (Default) Times New Roman, 12 pt